

# Does intermittency affect the inertial transfer rate in stationary isotropic turbulence?

S. R. Yoffe\* and W. D. McComb,  
 SUPA School of Physics and Astronomy,  
 Peter Guthrie Tait Road,  
 University of Edinburgh,  
 EDINBURGH EH9 3JZ.  
 Email: wdm@ph.ed.ac.uk

January 13, 2022

## Abstract

Direct numerical simulations of the forced Navier-Stokes equations were performed, in which each shell-averaged quantity evolved from a value appropriate to an initial Gaussian state, to fluctuate about a mean value. Once the transient had passed, mean values (and their associated statistics) were obtained by sampling the evolved time-series at intervals of the order of an eddy-turnover time. This was repeated for a range of Taylor-Reynolds numbers from 10.6 to 335.2. With increasing Reynolds number, our results for energy spectra, transfer spectra and inertial flux supported the Kolmogorov-Obukhov picture of turbulent energy transfer. In particular, we observed the onset of scale-invariance of the inertial flux, accompanied by the onset of the  $-5/3$  power law in the energy spectrum for the corresponding inertial range of wavenumbers. Detailed comparisons showed that our results were in agreement with those found in many other investigations. Flow visualization methods were used to study the internal intermittency. This phenomenon is seen in single realisations but was found to average out with increasing number of realisations under ensemble-averaging. Following a critical review of the literature relating to the controversy about intermittency effects versus finite-Reynolds number corrections, it was concluded that, for the case of stationary isotropic turbulence, internal intermittency cannot affect the Kolmogorov-Obukhov picture, as this is constructed entirely in terms of ensemble-averaged mean quantities.

---

\*SUPA Department of Physics, University of Strathclyde, John Anderson Building, 107 Rottenrow East. Glasgow G4 0NG.

# Contents

<b>1</b>	<b>Introduction</b>	<b>3</b>
1.1	A short statement of the problem . . . . .	4
1.2	The Kolmogorov-Obukhov theory of turbulence . . . . .	5
<b>2</b>	<b>The numerical simulation</b>	<b>7</b>
2.1	Details of the numerical method . . . . .	7
2.2	Summary of simulations carried out . . . . .	9
2.2.1	Notation and definitions . . . . .	9
2.2.2	Preliminary results . . . . .	11
<b>3</b>	<b>Properties of the ensemble</b>	<b>13</b>
3.1	The compensated energy spectrum . . . . .	13
3.2	Longitudinal velocity derivative skewness . . . . .	15
3.3	Dissipation-scaled energy spectrum . . . . .	15
3.4	Resolution of the small scales . . . . .	15
3.5	Isotropy . . . . .	16
<b>4</b>	<b>Results for scale-invariance and the Kolmogorov spectrum</b>	<b>18</b>
4.1	The Kolmogorov prefactor . . . . .	18
4.2	Reynolds number dependence of statistics . . . . .	19
<b>5</b>	<b>Results illustrating the nature of internal intermittency</b>	<b>22</b>
5.1	Visualisation of coherent structures . . . . .	22
5.1.1	Isovorticity . . . . .	22
5.1.2	The $Q$ -criterion . . . . .	23
5.1.3	Rate-of-strain . . . . .	24
5.2	Persistence of structure under averaging . . . . .	24
<b>6</b>	<b>Discussion: intermittency effects <i>versus</i> finite-Reynolds-number corrections</b>	<b>32</b>
6.1	Internal intermittency . . . . .	32
6.2	Cascade or vortex stretching? . . . . .	32
6.3	The Landau criticism of K41 and problems with averages . . . . .	34
6.4	The Kolmogorov (1962) theory: a critical view . . . . .	36
6.5	Anomalous exponents . . . . .	37
6.6	Theoretical and experimental support for Kolmogorov (1941) . . . . .	38
<b>7</b>	<b>Conclusion</b>	<b>41</b>

# 1 Introduction

In 2001, Lumley and Yaglom published an article ‘A Century of Turbulence’ [1]. After they had made it clear that neither author had been involved with turbulence for the entire century, their conclusions were bleak. We may quote from their Abstract, as follows:

*‘This field does not appear to have a pyramidal structure, like the best of physics. We have very few great hypotheses. Most of our experiments are exploratory experiments. What does this mean?’*

They go on to answer their own question:

*‘We believe that it means that, even after 100 years, turbulence studies are still in their infancy.’*

The passage of another two decades does not seem to have altered that conclusion, and even if we restrict our attention to isotropic turbulence — arguably the most fundamental branch of the subject — this is still characterised by various unresolved issues. For instance, we have the endlessly contentious problems posed by topics like the scaling of two-time correlations and the free decay of the total kinetic energy. In the latter case, there is often a failure to appreciate that the three distinct problems posed by the mathematical physics problem of free decay; the numerical simulation of free decay; and the decay of grid-generated turbulence are all, in principle, not quite the same problem. There is also a widespread belief that the infinite Reynolds number limit is the same thing as setting the viscosity to zero, accompanied it would appear by a belief in the failure of the continuum description of the fluid concerned. But, above all, there is the idea that the Komogorov ‘ $-5/3$ ’ spectrum is subject to intermittency corrections. From a fundamental view this is difficult to understand because Kolmogorov’s theory [2] was expressed in terms of the *mean* dissipation, which can hardly be affected by intermittency.

The trouble seems to be that Kolmogorov’s theory (K41, for brevity), despite its great pioneering importance, was an incomplete and indeed inconsistent theory. It was formulated in real space; where, although the energy transfer process can be loosely visualised from Richardson’s idea [3] of a cascade, the concept of such a cascade is not mathematically well defined. Also, having introduced the inertial range of scales, where the viscosity may be neglected, he characterised this range by the viscous dissipation rate, which is not only inconsistent but incorrect<sup>1</sup>. An additional complication, which undoubtedly plays a part, is that his theory was applied to turbulence in general. The basic idea was that the largest scales would be affected by the nature of the flow, but a stepwise cascade would result in smaller eddies being universal in some sense. That is, they would have much the same statistical properties, despite the different conditions of formation. In order to avoid uncertainties that can arise from this rather general idea, we will restrict our attention to stationary, isotropic turbulence in this article.

To make a more physical picture we have to follow Obukhov and work in  $k$ -space, with the Fourier transform  $\mathbf{u}(\mathbf{k}, t)$  of the velocity field  $\mathbf{u}(\mathbf{x}, t)$ . This procedure was introduced by Taylor, in order to allow the problem of isotropic turbulence to be formulated as one of statistical mechanics, with the Fourier components acting as the degrees of freedom. In this way, Obukhov identified the conservative, inertial flux of energy through the modes as being the key quantity determining the energy spectrum in the inertial range. It follows that, with the input and dissipation being negligible, the flux must be constant (i.e. independent of wavenumber) in

---

<sup>1</sup>In his exegesis of Kolmogorov’s theories, Batchelor [4] referred to ‘the constant rate at which each set (*sic*) passes to the next smaller neighbour’; but, in general, discussion and criticism of K41 continues to use the term ‘dissipation’.

the inertial range, with the extent of the inertial range increasing as the Reynolds number was increased. This was later recognized by Osager [5]. Later still, this property became widely known and for many years has been referred to by theoretical physicists as *scale invariance*<sup>2</sup>. It should be emphasised that the inertial flux is an average quantity, as indeed is the energy spectrum, and any intermittency effects present, which are characteristics of the instantaneous velocity field, will inevitably be averaged out. Of course, in stationary flows the inertial transfer rate is the same as the dissipation rate, but in non-stationary flows it is not.

This is not intended to minimise the importance of Kolmogorov’s pioneering work. It is merely that we will argue here that one also needs to consider Obukhov’s theory [6], with possibly also a later contribution from Onsager [5], in order to have a complete theoretical picture. In effect this seems to have been the view of the turbulence community from the late 1940s onwards. Discussion of turbulent energy transfer and dissipation in isotropic turbulence was almost entirely in terms of the spectral picture. It was not until the extensive measurements of higher-order structure functions by Anselmet *et al.* [7] that the real-space picture became of interest, along with the concept of *anomalous exponents*. To lay a foundation for the present work, we will first state the problem in a more succinct fashion and then consider the joint Kolmogorov-Obukhov picture in more detail.

## 1.1 A short statement of the problem

By restricting our attention to stationary, isotropic turbulence, we rule out effects due to mean shear, system rotation, density stratification, and so on. This leaves us with a stark choice: deviations from Kolmogorov’s predictions for the energy spectrum (or second-order structure function) must be due either to the Reynolds number being finite (K41 is based on an assumption of very large Reynolds numbers)<sup>3</sup> or to the effects of internal intermittency, as was suggested later on by Kolmogorov in 1962.

Over the last few decades a veritable industry has grown up, based on the search for so-called *intermittency corrections*. Recently it has been dominated by multi-scale or multifractal models of turbulence; but this topic now seems less popular. Such activity finds a sympathetic audience, because many people seem to see the K41 picture as being counter-intuitive, when one considers aspects of turbulence such as vortex-stretching, localness, intermittency and the taking of averages.

Running counter to this belief in ‘intermittency corrections’ (or, increasingly, ‘anomalous exponents’) which has been dominant in recent times, there is a growing view (see references [8]–[14]) that K41 is an asymptotic theory, valid in the limit of infinite Reynolds number. In this school of thought, any deviations from K41 are due to finite viscosity. As a result, opinion in the turbulence community is deeply divided on this fundamental issue. Here we will begin by giving a succinct statement of the situation.

As is well known, in 1941, Kolmogorov [2, 15] gave two different derivations of his famous result for the second-order structure function<sup>4</sup>:

$$S_2 = C\varepsilon^{2/3}r^{2/3}, \quad (1)$$

for  $l < r < L$ , where  $l$  is a measure of the scale at which viscous effects begin to dominate (*i.e.* the internal scale),  $L$  is a measure of the large scales of the system (*i.e.* the external scale) and

---

<sup>2</sup>Scale invariance is a general mathematical property and can refer to various things in turbulence research. It simply means that something which might depend on an independent variable, in either real space or wavenumber space, is in fact constant.

<sup>3</sup>Strictly, we should also bear in mind the possibility of the persistence of input/forcing effects.

<sup>4</sup>These are often referred to as K41A and K41B, respectively.



the prefactor takes the value  $C \simeq 2$ . As is equally well known, the corresponding result for the energy spectrum in wavenumber is

$$E(k) = \alpha \varepsilon^{2/3} k^{-5/3}, \quad (2)$$

where the prefactor  $\alpha$  is widely known as the *Kolmogorov constant* and takes a value of about  $\alpha = 1.6$ . As pointed out earlier, this result may be attributed to Obukhov [6] and Onsager [5]. Despite this, for our present purposes we will follow standard practice and refer to both (1) and (2) as K41.

Shortly after this work was published, it was criticised by Landau (see the footnote on page 126 of [16]). Kolmogorov [17] interpreted this criticism as a need to treat the dissipation rate as a variable; and, working with its average taken over a sphere of radius  $r$ , concluded that the right hand side of equation (1) should be multiplied by a factor  $(L/r)^\mu$ , where  $\mu$  is often referred to nowadays as an *intermittency correction*. We will refer to this later theory as K62.

That development gave rise to further attempts by other workers to obtain a value for  $\mu$ . As a result, for many years K41 has had a question mark hanging over its status as a theory of inertial-range turbulence. From our present point of view, the question may be posed as: is there an intermittency correction to the Kolmogorov spectrum?

## 1.2 The Kolmogorov-Obukhov theory of turbulence

For completeness, we should begin by mentioning that Kolmogorov also used the Kármán-Howarth equation, which is the energy balance equation connecting the second- and third-order structure functions, to derive the so-called ‘4/5’ law for the third-order structure function [15]. This procedure amounts to a *de facto* closure, as the time-derivative is neglected (an exact step in our present case) and the term involving the viscosity vanishes in the limit of infinite Reynolds number. This is often described as ‘*the only exact result in turbulence theory*’; but increasingly it is being said, perhaps more correctly, to be ‘the only *asymptotically* exact result in turbulence’.

As part of this work [15], Kolmogorov also assumed that the skewness was constant; and this provided a relationship between the second- and third-order structure functions which recovered the ‘2/3’ law. It is interesting to note that Lundgren [13] used the method of matched asymptotic expansions to obtain both the ‘4/5’ and ‘2/3’ laws, without having to make any assumption about the skewness. His work also offered a way of estimating the extent of the inertial range in real space.

The Kármán-Howarth equation is local in the independent variables and therefore does not describe an energy cascade. In contrast, the Lin equation (which is just its Fourier transform) shows that all the degrees of freedom in turbulence are coupled together. It takes the form, for the energy spectrum  $E(k, t)$ , in the presence of an input spectrum  $W(k)$ :

$$\frac{\partial E(k, t)}{\partial t} = W(k) + T(k, t) - 2\nu_0 k^2 E(k, t), \quad (3)$$

where  $\nu_0$  is the kinematic viscosity and the transfer spectrum  $T(k, t)$  is given by

$$\begin{aligned} T(k, t) &= 2\pi k^2 \int d^3 j \int d^3 l \delta(\mathbf{k} - \mathbf{j} - \mathbf{l}) M_{\alpha\beta\gamma}(\mathbf{k}) \\ &\times \{C_{\beta\gamma\alpha}(\mathbf{j}, \mathbf{l}, -\mathbf{k}; t) - C_{\beta\gamma\alpha}(-\mathbf{j}, -\mathbf{l}, \mathbf{k}; t)\}, \end{aligned} \quad (4)$$

with

$$M_{\alpha\beta\gamma}(\mathbf{k}) = -\frac{i}{2} [k_\beta P_{\alpha\gamma}(\mathbf{k}) + k_\gamma P_{\alpha\beta}(\mathbf{k})], \quad (5)$$

and the projector  $P_{\alpha\beta}(\mathbf{k})$  is:

$$P_{\alpha\beta}(\mathbf{k}) = \delta_{\alpha\beta} - \frac{k_\alpha k_\beta}{|\mathbf{k}|^2}, \quad (6)$$

where  $\delta_{\alpha\beta}$  is the Kronecker delta, and the third-order moment  $C_{\beta\gamma\alpha}$  here takes the specific form:

$$C_{\beta\gamma\alpha}(\mathbf{j}, \mathbf{l}, -\mathbf{k}; t) = \langle u_\beta(\mathbf{j}, t) u_\gamma(\mathbf{l}, t) u_\alpha(-\mathbf{k}, t) \rangle. \quad (7)$$

At this stage we will also define the flux of energy  $\Pi(\kappa, t)$  due to inertial transfer through the mode with wavenumber  $k = \kappa$ . This is given by:

$$\Pi(\kappa, t) = \int_\kappa^\infty dk T(k, t). \quad (8)$$

Further discussion and details may be found in Section 4.2 of the book [18].

We now have a rather simple picture. The form of the input spectrum should be chosen to be peaked near the origin, such that higher wavenumbers are driven by inertial transfer, with energy being dissipated locally by the viscosity. We can define the rate at which stirring forces do work on the system by:

$$\int_0^\infty W(k) dk = \varepsilon_W. \quad (9)$$

Obukhov's idea of the constant inertial flux can be expressed as follows. As the Reynolds number is increased, the transfer rate, as given by equation (8), must also increase and reach a maximum value which, in turn must be equal to the viscous dissipation. Thus we introduce the symbol  $\varepsilon_T$  for the maximum inertial flux as:

$$\varepsilon_T = \Pi_{\max}, \quad (10)$$

and for stationary turbulence at sufficiently high Reynolds number, we have the limiting condition:

$$\varepsilon = \varepsilon_T = \varepsilon_W. \quad (11)$$

Thus the loose idea of a local cascade involving eddies in real space is replaced by the precisely formulated concept of scale invariance of the inertial flux in wavenumber space.

Our main purpose in the present work is to examine this concept of scale invariance in wavenumber space and also the effect on the intermittency of the averaging process. The paper is organised as follows:

**Section 2** We begin by describing our numerical methods and summarising the simulations which we carried out.

**Section 3** The use of a statistical ensemble, in addition to the usual shell averaging, is discussed with particular reference to isotropy, the evaluation of errors and the resolution of both small and large scales.

**Section 4** A detailed assesment is made of the onset of scale invariance of the energy flux and also the Kolmogorov spectrum, for a range of wavenumbers.

**Section 5** We make use of flow visualization in real space to assess the effect of ensemble-averaging on the internal intermittency.

**Section 6** In order to provide a context for our results, we discuss various recent investigations, both theoretical and experimental, which support the K41 theory in the limit of infinite Reynolds numbers.

## 2 The numerical simulation

Over the last decade or more, we have been using direct numerical simulation along with analytical methods to study outstanding problems and unresolved issues in isotropic turbulence. This has involved carrying out simulations of the Navier-Stokes equation, based on an initially Gaussian field, with a prescribed initial spectrum, and allowing a turbulent velocity field to develop with time for both free decay and forced simulations.

The initial spectrum was taken to be a standard form given by:

$$E(k, 0) = C_1 k^{C_2} \exp(-C_3 k^{C_4}), \quad (12)$$

where the constants  $C_1 - C_4$  have to be chosen. As we require the initial spectrum to be peaked near the origin, so that the excitation of higher wavenumbers is purely by nonlinear transfer, it is usual to be influenced by the low- $k$  expansion of the spectrum, thus:

$$E(k, 0) = Ak^2 + Bk^4 + \mathcal{O}(k^6). \quad (13)$$

For decades there has been controversy over whether the spectrum should start off as  $k^2$  or  $k^4$ , so like others in the field we have used both forms. However, more recently it has been shown that  $A = 0$  is an exact result [19], and accordingly we now only consider trial spectra that begin as  $k^4$ .

We began by studying freely decaying turbulence, and showed that the so-called Taylor dissipation surrogate was in fact a better surrogate for the nonlinear energy transfer and only became equal to the dissipation when the Reynolds number was high enough for spectral scale invariance to be present [20]. Later we studied the onset of Navier-Stokes turbulence in free decay from arbitrary initial conditions and proposed new onset criteria for this [21]. For forced stationary turbulence, we showed that correcting for systematic errors led to the canonical result  $n = 2/3$  for the exponent of the second-order structure function as the asymptotic result for large Reynolds numbers [22]. We have also shown that in stationary turbulence the dimensionless dissipation rate asymptotes to a universal value at large Reynolds numbers [23]. In this work, the results of the simulation supplemented an analysis which was asymptotically exact in the limit of large Reynolds numbers. Lastly, we found that at very low Reynolds numbers, a forced simulation undergoes a symmetry-breaking phase transition to a self-organised state [24]. Our general approach has also been extended to magnetohydrodynamic turbulence, e.g. see [25], [26].

Our simulations have been well validated by means of extensive and detailed comparison with the results of other investigations. Further details of the performance of our code may be found in the thesis by Yoffe [27], along with a direct comparison with the freely-available pseudospectral code `hit3d` [28, 29]. The Taylor-Green vortex was simulated as a benchmarking problem and our results were in good agreement with those of Brachet *et al* [30]. Furthermore our data reproduces the characteristic behaviour for the plot of the dimensionless dissipation rate  $C_\epsilon$  against  $R_\lambda$  [18], and agree closely with other representative results in the literature, such as the work by Wang, Chen, Brasseur and Wyngaard [31], Cao, Chen and Doolen [32], Gotoh, Fukayama and Nakano [33], Kaneda, Ishihara, Yokokawa, Itakura and Uno [34], Donzis, Sreenivasan and Yeung [35] and Yeung, Donzis and Sreenivasan [36], although there are some differences in forcing methods.

### 2.1 Details of the numerical method

We used a pseudospectral direct numerical simulation (DNS), with full de-aliasing implemented by truncation of the velocity field according to the two-thirds rule [37]. Time advancement for

the viscous term was performed exactly using an integrating factor, while the non-linear term was stepped forward in time using Heun's method [38], which is a second-order predictor-corrector routine. Each simulation was started from a Gaussian-distributed random field with a specified energy spectrum, which followed  $k^4$  for the low- $k$  modes. Measurements were taken after the simulations had reached a stationary state. The system was forced by negative damping, with the Fourier transform of the force  $\mathbf{f}$  given by

$$\begin{aligned}\mathbf{f}(\mathbf{k}, t) &= (\varepsilon_W/2E_f)\mathbf{u}(\mathbf{k}, t) \quad \text{for } 0 < |\mathbf{k}| < k_f; \\ &= 0 \quad \text{otherwise,}\end{aligned}\tag{14}$$

where  $\mathbf{u}(\mathbf{k}, t)$  is the instantaneous velocity field (in wavenumber space). The highest forced wavenumber,  $k_f$ , was chosen to be  $k_f = 2.5k_{\min}$ , where  $k_{\min} = 2\pi/L_{\text{box}} = 1$  is the lowest resolved wavenumber. As  $E_f$  was the total energy contained in the forcing band, this ensured that the energy injection rate was  $\varepsilon_W = \text{constant}$ . It is worth noting that no method of energy injection employed in the numerical simulation of isotropic turbulence is experimentally realizable. The present method of negative damping has also been used in other investigations [39, 40, 41, 34, 42], albeit not necessarily such that  $\varepsilon_W$  is maintained constant (and note the theoretical analysis of this type of forcing by Doering and Petrov [43]). Also, note that the correlation between the force and the velocity is restricted to the very lowest wavenumbers.

For each Reynolds number studied, we used the same initial spectrum and input rate  $\varepsilon_W$ . The initial spectrum took the form:

$$E(k, 0) = C_1 k^4 \exp(-C_3 k^2),\tag{15}$$

which is (12) with  $C_2 = 4$  and  $C_4 = 2$ . The other constants were given the values:  $C_1 = 0.001702$  and  $C_3 = 0.8$ . The only initial condition changed from one run (i.e. value of the Reynolds number) to another was the value assigned to the kinematic viscosity. Once the initial transient had passed, the velocity field was sampled every half a large-eddy turnover time,  $\tau = L/U$ , where  $L$  denotes the average integral scale and  $U$  the rms velocity. The ensemble populated with these sampled realizations was used, in conjunction with the usual shell averaging, to calculate statistics.

Simulations were run using lattices of size  $64^3$ ,  $128^3$ ,  $256^3$ ,  $512^3$  and  $1024^3$ , with corresponding Reynolds numbers ranging from  $R_\lambda = 10.6$  up to  $335.2$ . The smallest wavenumber was  $k_{\min} = 2\pi/L_{\text{box}} = 1$  in all simulations, while the maximum wavenumber satisfied  $k_{\max}\eta \geq 1.30$  for all runs except that in which  $R_\lambda = 335.2$  which satisfied  $k_{\max}\eta \geq 1.01$ , where  $\eta$  is the Kolmogorov dissipation lengthscale.<sup>5</sup> The integral scale,  $L$ , was found to lie between  $0.17L_{\text{box}}$  and  $0.23L_{\text{box}}$ .

It can be seen in Figure 2 of McComb, Hunter and Johnston [44] that a small-scale resolution of  $k_{\max}\eta > 1.6$  is desirable in order to capture the relevant dissipative physics. Evidently, this would restrict the attainable Reynolds number of the simulated flow, and the reference suggests that  $k_{\max}\eta \geq 1.3$  would still be acceptable (containing  $\sim 99.5\%$  of dissipative dynamics [27]). In contrast, at  $k_{\max}\eta \simeq 1$  a non-negligible part of the dissipation is left out of account. Many high resolution simulations of isotropic turbulence try to attain Reynolds numbers as high as possible and thus opt for minimal resolution requirements. In this paper the simulations have been conducted following a more conservative approach, where the emphasis has been put on better resolving the physical processes, thus necessarily compromising to some extent on Reynolds number. Large-scale resolution has only relatively recently received attention in the literature. As mentioned above, the largest scales of the flow are smaller than a quarter of the

---

<sup>5</sup>Note that a subsequent run at  $2048^3$  achieved  $R_\lambda = 435.2$  and satisfied  $k_{\max}\eta \geq 1.30$ . This was reported in [22], but was not used in the work presented here.

simulation box size. Further discussion is given later on in Section 3.4, where we consider the dissipation requirements in more detail.

## 2.2 Summary of simulations carried out

We begin by briefly summarising our previous discussion before providing the relevant definitions, and the details of the simulations.

The time evolution of forced isotropic turbulence was simulated for a range of Taylor-Reynolds numbers,  $8.70 \leq R_\lambda \leq 335.2$ . At each of the Reynolds numbers studied, the system was initialised as a Gaussian random field, using an initial spectrum with  $k^4$  as its low  $k$  behaviour, and allowed to reach a steady-state solution of the Navier-Stokes equations for shell-averaged quantities. Once this initial transient period had passed, the velocity field was sampled at intervals corresponding to one half of a large eddy turnover time,  $\tau = L/u$ , to create a set of realisations making up a statistical ensemble. As well as having been shell-averaged, the energy and transfer spectra were also averaged over this ensemble and used to calculate the statistics of the velocity field.

### 2.2.1 Notation and definitions

The various parameters calculated either during the simulation, or from the spectra after the simulation, include:

**Total energy** This is found by integrating the energy spectrum over all  $k$ :

$$E(t) = \int dk E(k, t). \quad (16)$$

**Root-mean-square (rms) velocity** A characteristic velocity scale is found from the total energy, since the total energy is proportional to the velocity squared:

$$E(t) = \frac{1}{2} \langle u^2(\mathbf{x}, t) \rangle = \frac{1}{2} [\langle u_x^2(\mathbf{x}, t) \rangle + \langle u_y^2(\mathbf{x}, t) \rangle + \langle u_z^2(\mathbf{x}, t) \rangle] . \quad (17)$$

By assuming isotropy, we have  $\langle u_x^2(\mathbf{x}, t) \rangle = \langle u_y^2(\mathbf{x}, t) \rangle = \langle u_z^2(\mathbf{x}, t) \rangle = u^2$  so that  $E(t) = \frac{3}{2} u^2$ , or

$$u(t) = \sqrt{\frac{2}{3} E(t)} . \quad (18)$$

**Dissipation spectrum** The dissipation spectrum has the form

$$D(k, t) = 2\nu_0 k^2 E(k, t) , \quad (19)$$

so is readily found from the energy spectrum.

**Dissipation rate** The dissipation rate is the integral of the dissipation spectrum:

$$\varepsilon(t) = \int dk D(k, t) . \quad (20)$$

**Integral scale** This gives a characteristic length-scale of the system based on large-scale structures. It was initially introduced with model fits to the correlation function  $f(r) \sim e^{-r/L}$ . It is defined in Fourier space as

$$L(t) = \frac{3\pi}{4E(t)} \int dk \frac{E(k)}{k} . \quad (21)$$

**Taylor micro-scale** Another important length-scale, this time characterising the small-scale structures of the system. It is found as:

$$\lambda(t) = \left( \frac{10\nu_0 E(t)}{\varepsilon(t)} \right)^{1/2} = \left( \frac{15\nu_0 u^2(t)}{\varepsilon(t)} \right)^{1/2} . \quad (22)$$

**The Reynolds numbers** In general it is defined as:

$$Re = \frac{Ul}{\nu_0} , \quad (23)$$

where  $U$  and  $l$  are some characteristic (possibly time-dependent) velocity- and length-scales and  $\nu_0$  is the kinematic viscosity. In this investigation we use the integral-scale Reynolds number  $R_L = uL/\nu_0$  and the Taylor-Reynolds number  $R_\lambda = u\lambda/\nu_0$ .

**The Kolmogorov scale** The Kolmogorov length-scale gives the approximate scale at which viscous effects become important and is given by:

$$\eta(t) = \left( \frac{\nu_0^3}{\varepsilon(t)} \right)^{1/4} . \quad (24)$$

**Longitudinal velocity derivative skewness** Also referred to as simply the skewness, the longitudinal velocity derivative skewness is one of the most sensitive parameters in quantifying turbulence. In real space, it is defined as:

$$S(t) = \frac{\langle (\partial_1 u_1(\mathbf{x}, t))^3 \rangle}{\langle (\partial_1 u_1(\mathbf{x}, t))^2 \rangle^{3/2}} , \quad (25)$$

where  $\partial_1 = \partial/\partial x_1$ , or in Fourier space as:

$$S(t) = \frac{2}{35} \left( \frac{\lambda(t)}{u(t)} \right)^3 \int dk \, k^2 T(k, t) . \quad (26)$$

It should be noted that pseudospectral methods have access to both of these methods, and there is often a discrepancy between what should be equivalent results.

**Structure functions** Structure functions are found in configuration space by considering the correlations of the difference between two points. The  $n^{th}$ -order longitudinal structure function is defined as:

$$S_n(r) = \left\langle \left[ \delta \mathbf{u}(\mathbf{r}) \cdot \hat{\mathbf{r}} \right]^n \right\rangle = \left\langle \left[ (\mathbf{u}(\mathbf{x} + \mathbf{r}, t) - \mathbf{u}(\mathbf{x}, t)) \cdot \hat{\mathbf{r}} \right]^n \right\rangle . \quad (27)$$

**Dissipative wavenumber** The dissipation wavenumber  $k_d$  is the reciprocal of the Kolmogorov microscale. To quantify how well resolved a computation is, we consider the lowest wavenumber  $k_{\text{diss}}$  such that

$$\int_0^{k_{\text{diss}}} dk \, 2\nu_0 k^2 E(k, t) \geq 0.995\varepsilon . \quad (28)$$

That is, the wavenumber up to which 99.5% of the dissipation is accounted for. This should satisfy  $k_{\text{diss}} < k_{\text{max}}$  for the simulation to be well resolved.

ID	$R_L$	$R_\lambda$	$u$	$L$	$\lambda$	$\varepsilon$	$\varepsilon_T$	$S$	$k_{\text{diss}}$	$k_d$	$\Pi(0) (\times 10^{-9})$
f64d	10.6	8.70	0.441	2.163	1.777	0.083	0.026	0.566	5	3	62.9
f64c	12.8	9.91	0.440	2.041	1.578	0.081	0.031	0.615	6	4	5.20
f64a	19.0	13.9	0.485	1.956	1.435	0.086	0.037	0.583	7	5	-42.9
f64b	39.5	24.7	0.523	1.512	0.943	0.092	0.060	0.554	13	10	-64.0
f128a	82.7	42.5	0.581	1.442	0.733	0.094	0.079	0.540	22	18	-73.9
f128b	88.2	44.0	0.578	1.374	0.686	0.096	0.083	0.533	24	19	60.1
f128c	101.4	48.0	0.586	1.383	0.655	0.096	0.084	0.535	26	21	-46.5
f128d	105.7	49.6	0.579	1.279	0.600	0.098	0.088	0.531	29	23	20.7
f128e	158.6	64.2	0.607	1.307	0.529	0.099	0.092	0.529	38	30	-5.10
f256a	284.6	89.3	0.600	1.185	0.372	0.098	0.095	0.522	64	50	-58.1
f256b	360.1	101.3	0.607	1.187	0.334	0.099	0.096	0.521	76	59	37.5
f256c	432.6	113.3	0.626	1.243	0.326	0.100	0.099	0.525	80	65	-69.7
f512a	1026	176.9	0.626	1.181	0.204	0.102	0.100	0.537	162	129	11.8
f512b	1373	203.7	0.608	1.129	0.167	0.099	0.098	0.518	168	168	-30.9
f512c	81.5	41.8	0.581	1.403	0.720	0.097	0.082	0.535	22	18	-26.6
f512d	146.5	60.8	0.589	1.243	0.516	0.098	0.093	0.525	38	30	38.0
f512e	287.8	89.4	0.605	1.189	0.369	0.101	0.096	0.525	65	51	-75.7
f512f	436.3	113.0	0.620	1.267	0.328	0.096	0.096	0.535	83	64	22.1
f512g	785.2	153.4	0.626	1.255	0.245	0.098	0.095	0.541	132	99	70.9
f1024a	2415	276.2	0.626	1.158	0.132	0.100	0.100	0.557	323	247	-4.40
f1024b	3535	335.2	0.626	1.130	0.107	0.102	0.102	0.541	337	337	-34.3

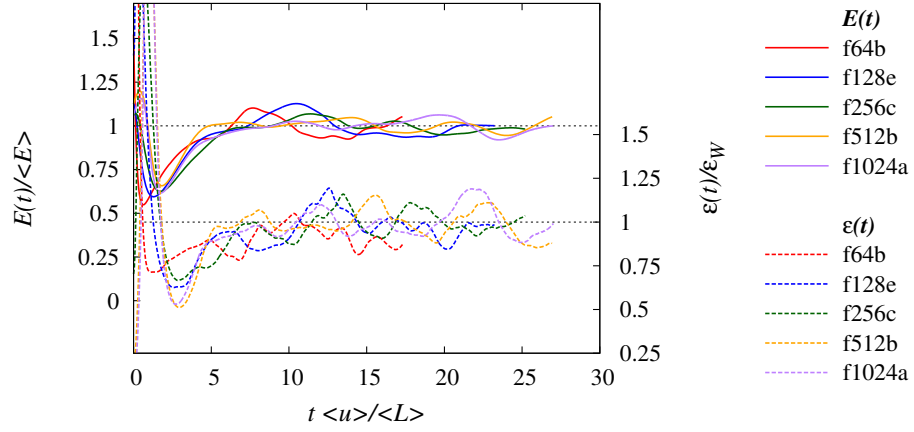
Table 1: Summary of the mean statistics for the simulations.

## 2.2.2 Preliminary results

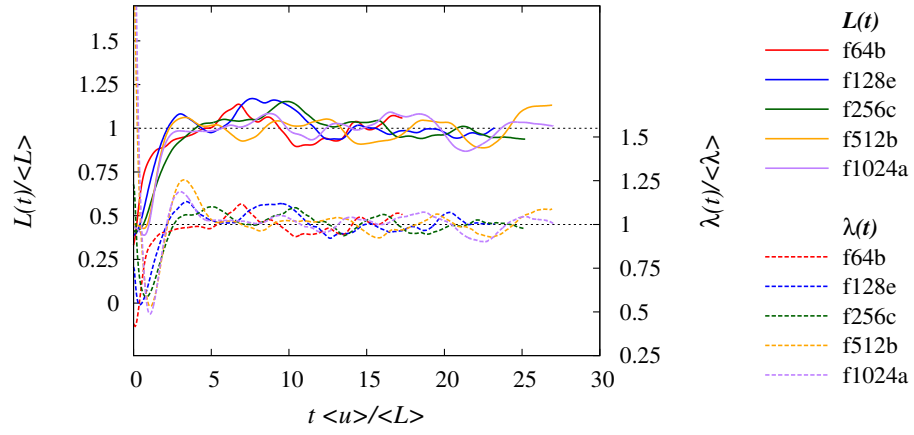
Table 1 summarises the mean values of the most important statistical quantities in our simulations. Figure 1 shows the evolution of some of these key parameters as the simulation progresses from its Gaussian initial condition to the steady state. The quantities have been scaled by their ensemble-averaged mean value. Note that each sub-figure shows two variables, one of which is plotted using continuous lines and the other using dotted lines. The left hand ordinate shows values for the continuous lines, whereas the right hand ordinate is for the dotted lines. The key for both types of line may be found to the right hand side of the figure.

As can be seen, after  $t \sim 10\langle L \rangle / \langle u \rangle$  most simulations have settled to their evolved state. The figures also highlight the fact that stationarity is a statistical concept. Fluctuations around the mean are expected, and present in the system, but they should vanish under further (time or ensemble) averaging. An analogy can be drawn with the canonical ensemble in statistical mechanics: the turbulent system fluctuates about mean values determined by the rate at which the system is driven by the energy input.

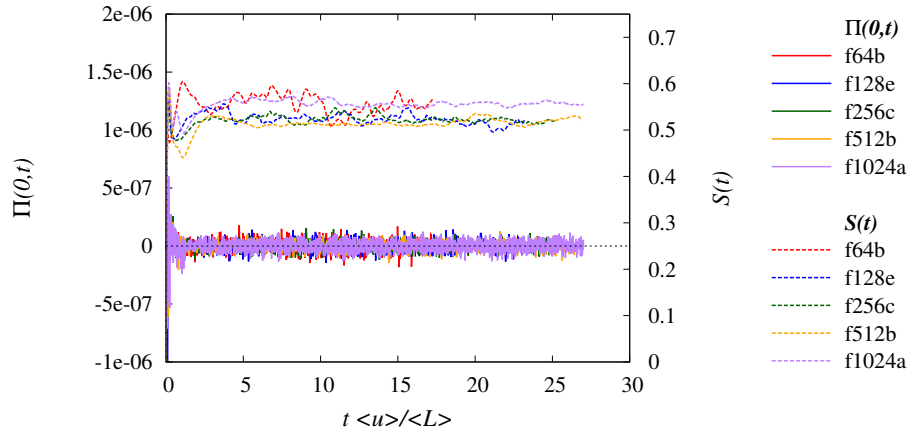
The integral over the transfer spectrum,  $\Pi(0, t)$ , is shown in figure 1(c) and can be seen to fluctuate around zero. The time-averaged values, given in table 1, show  $\Pi(0)$  to be consistently of order  $10^{-8}$  or smaller, indicating that the non-linear term is conserving energy. We shall expand on the properties of the statistical ensemble in the next section.



(a) Fluctuation of energy  $E$  and dissipation rate  $\varepsilon$ .



(b) Fluctuation of the integral length-scale  $L$  and the Taylor microscale  $\lambda$ .



(c) Fluctuation of skewness factor  $S$  and the transfer power  $\Pi(0, t)$ .

Figure 1: Time variation of key parameters for forced turbulence. Parts (a) and (b) are scaled by their steady-state mean value.



### 3 Properties of the ensemble

Shell-averaging was used to obtain time-varying statistics such as the fluctuation of total energy or the dissipation rate. These quantities were presented as time series. For stationary turbulence, once it reaches an evolved state, rather than run multiple simulations, an ensemble can be generated by sampling the field at various times. If the sample time between realisations is longer than the typical correlation time scales of the system, we can consider the times to be uncorrelated realisations of the flow. From this new ensemble, we can calculate a single mean value for each of various parameters of the stationary flow, along with their associated error.

First, we must discard the transient data collected while our system evolved from its initial condition into a stationary solution of the Navier-Stokes equation. Typically, this takes around 10 eddy turnover times. The remaining data is then sampled every  $\Delta t$  and used to calculate a mean value. Here,  $\Delta t$  should be of the order of  $\tau = L/u$ , the eddy turnover time, and in practice we found that  $\Delta t = \tau/2$  was sufficient. For the simulations in this work, we collected data for at least  $15\tau$  after the transition period. The ensemble-averaged value for the parameter  $A$  was then calculated as

$$\langle A \rangle = \frac{1}{T} \sum_{t_i \in \mathbb{T}} A(t_i) , \quad (29)$$

where  $T$  is the number of realisations in our ensemble,  $\mathbb{T}$ . An estimate of the error is given by the standard deviation,

$$\sigma_A^2 = \langle A^2 \rangle - \langle A \rangle^2 , \quad (30)$$

although we occasionally refer to the *standard error* on the mean, denoted  $\hat{\sigma}$ , where

$$\hat{\sigma} = \frac{\sigma}{\sqrt{T}} . \quad (31)$$

In order to establish the reliability of our code, we compared our results for certain key parameters with representative values in the field, as described in the following subsections.

#### 3.1 The compensated energy spectrum

Rearranging the Kolmogorov (K41) energy spectrum in terms of a wavenumber dependent  $\alpha(k)$  gives the *compensated* energy spectrum,

$$\alpha(k) = \varepsilon^{-2/3} k^{5/3} E(k) . \quad (32)$$

Regions in which this spectrum is flat thus take the Kolmogorov form,  $k^{-5/3}$ , with  $\alpha = \text{constant}$ . Figure 2 shows the compensated energy spectrum for an  $N = 1024$  simulation. The spectrum has been ensemble-averaged with  $\Delta t = \tau$ , allowing us to plot an estimate of the error.

As noted by Yeung and Zhou [45], there appear to be two plateaus: one at lower  $k$  and one at medium  $k$ . In the paper, the authors show how the location of the inertial range has been misidentified in many numerical simulations, causing the value of  $\alpha$  to be overestimated. They present arguments for the plateau at lower  $k$  corresponding to the actual inertial range. This is based on the peak of the dissipation spectrum coinciding with the higher plateau, hence it cannot correspond to inertial behaviour. This is also observed in our data, with the peak of the dissipation spectrum at  $k_p \sim 43$ , indicated in figure 2. Ishihara, Gotoh and Kaneda [46] also provide a discussion of this mis-identification.

To make an estimate for the value of the constant  $\alpha$ , we resort to the scaled transport power spectrum. As discussed earlier, in the inertial subrange of wavenumbers energy is transferred at the dissipation rate, such that the flux through a wavenumber  $k$  satisfies

$$\Pi(k, t) = \varepsilon(t) , \quad (33)$$

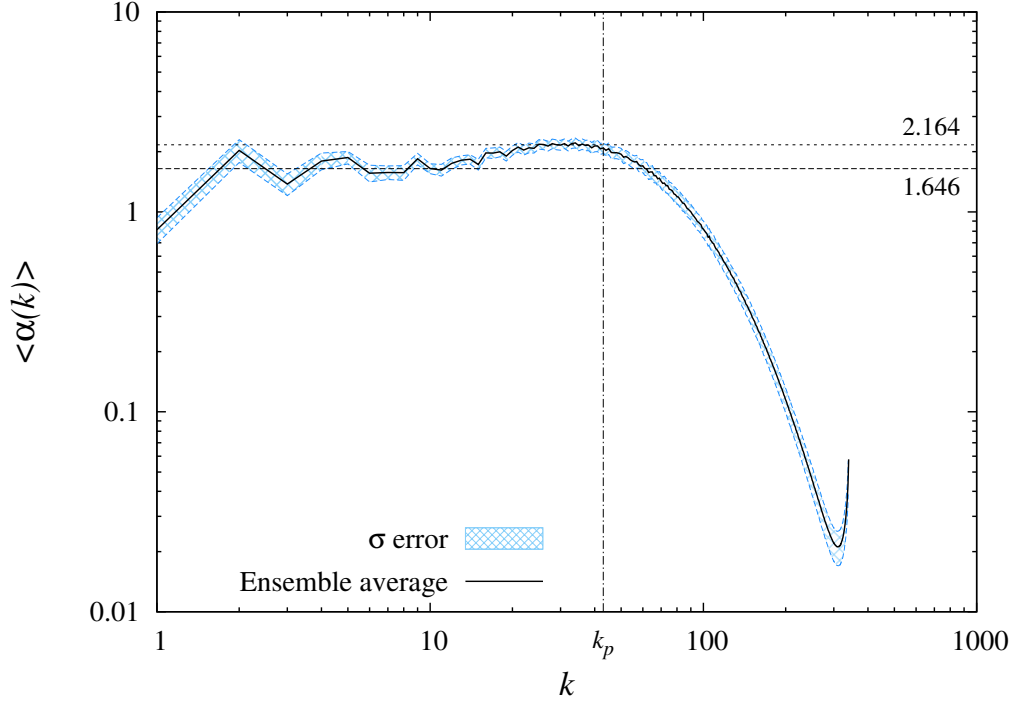


Figure 2: Ensemble-averaged compensated energy spectrum for  $R_\lambda \sim 280$ . (—) Averaged value of  $\alpha$ . (···) Anomalous plateau. (— · —)  $k_p \sim 43$ .

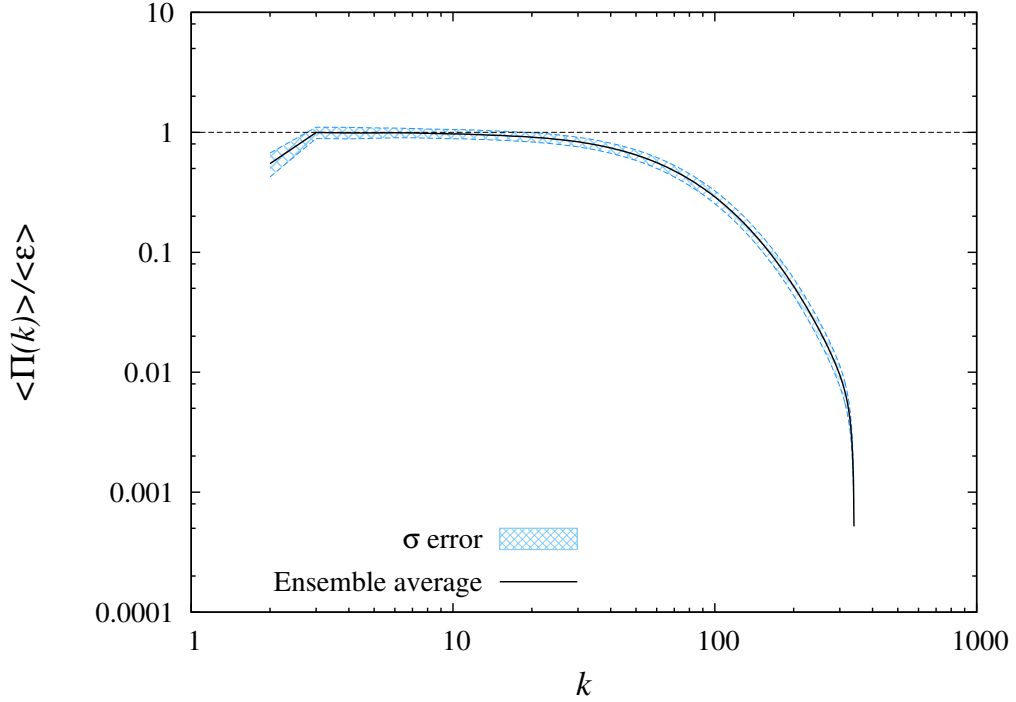


Figure 3: Ensemble-averaged scaled transport power spectrum for  $R_\lambda \sim 280$ .

making  $\langle \Pi(k) \rangle / \varepsilon$  a simple test for an inertial range. In figure 3, this can be seen to be unity for the range  $3 \leq k \leq 7$ , corresponding to the lower  $k$  plateau in figure 2. To obtain a mean value for this plateau, we averaged over the range to find the value

$$\alpha = 1.646 \pm 0.144 . \quad (34)$$

This value is highlighted in figure 2 by the dashed line, along with the value corresponding to the ‘anomalous’ plateau of 2.164 (dotted line).

Ishihara *et al.* [46] found  $\alpha = 1.5 - 1.7$  in their high- $R_\lambda$  simulations, placing our result within their range. In fact, studying the data found in Gotoh and Fukayama [47], one finds the value for their most similar Reynolds number,  $R_\lambda = 284$ , to be 1.64, in good agreement with the above. They quote an average value of  $\alpha = 1.65 \pm 0.05$ , and our own result agrees with this within one error unit. Yeung and Zhou [45] found a value of 1.62 for  $R_\lambda = 240$ . Note that the Kolmogorov constant can be measured from one- or three-dimensional energy spectra using the relation  $\alpha = (55/18)C_1$ , where  $C_1$  is measured from one-dimensional spectra [45]. Comparison can then also be made to the experimental value obtained by Sreenivasan [48] of  $C_1 = 0.53 \pm 0.055$  which gives  $\alpha = 1.62 \pm 0.17$ . Mydlarski and Warhaft [49] found the experimental value  $C_1 = 0.51$ , giving  $\alpha = 1.56$ . Further values for comparison obtained using direct numerical simulation and large-eddy simulation can be found in [45, 47, 31].

### 3.2 Longitudinal velocity derivative skewness

The skewness was computed in both real and Fourier space to obtain the values

$$S_x = 0.551 \pm 0.015 \quad \text{and} \quad S_k = 0.557, \quad (35)$$

respectively. The Fourier-space result has been calculated using the ensemble-averaged transfer spectrum, and as such it is difficult to associate an error with it. However, agreement with the real-space result is good.

This can be compared to other stationary simulations such as Ishihara *et al.* [46], who obtained  $S \sim 0.5$ , or Machiels [40] who quoted a result of  $S = 0.51$  for  $R_\lambda \simeq 190$ . Vincent and Meneguzzi [50] found a value of  $S = 0.5$  for  $R_\lambda \sim 150$ , which is the same as Kerr [51] for  $R_\lambda < 80$ . Gotoh, Fukayama and Nakano [33] performed a series of simulations on  $512^3$  and  $1024^3$  grids. For  $R_\lambda = 284$ , the closest Reynolds number to that used here, they found  $S = 0.531$ . The average value of their  $R_\lambda = 284$  and 381 runs gives  $S = 0.553$ . Jiménez, Wray, Saffman and Rogallo [39] obtained  $S = 0.525$  for  $R_\lambda = 168.1$ , while Wang, Chen, Brasseur and Wyngaard [31] found a value of  $S = 0.545$  for the largest forced run with  $R_\lambda = 195$ . Sreenivasan and Antonia [52] comment on skewness increasing monotonically with Reynolds number and present a collection of data from DNS and experiment to support this. This can also be observed in [53].

### 3.3 Dissipation-scaled energy spectrum

She, Chen, Doolen, Kraichnan and Orszag [54] found that energy spectra taken at various Reynolds numbers collapse when scaled on the peak of the dissipation spectrum; that is,  $k/k_p$  and  $E(k)/E(k_p)$ . The authors presented the collapse of DNS for Reynolds numbers  $R_\lambda \sim 70$  to 200, along with experimental data. In figure 4 we plot our own DNS results for two Reynolds numbers, along with data points from Vincent and Meneguzzi [50] for  $R_\lambda = 150$  for comparison. Note that the points have been extracted by hand from their figure. The data is seen to collapse well. The error shown is that for  $R_\lambda = 276$ .

### 3.4 Resolution of the small scales

A general rule for DNS is that one must satisfy  $k_{\max}\eta > 1$ , with  $k_{\max}\eta = 1$  being regarded as only partially resolved. It has been suggested that it is actually necessary to satisfy  $k_{\max}\eta > 1.5$  to capture the relevant dynamics [44]. Therefore, a series of ‘highly resolved’ runs was performed,

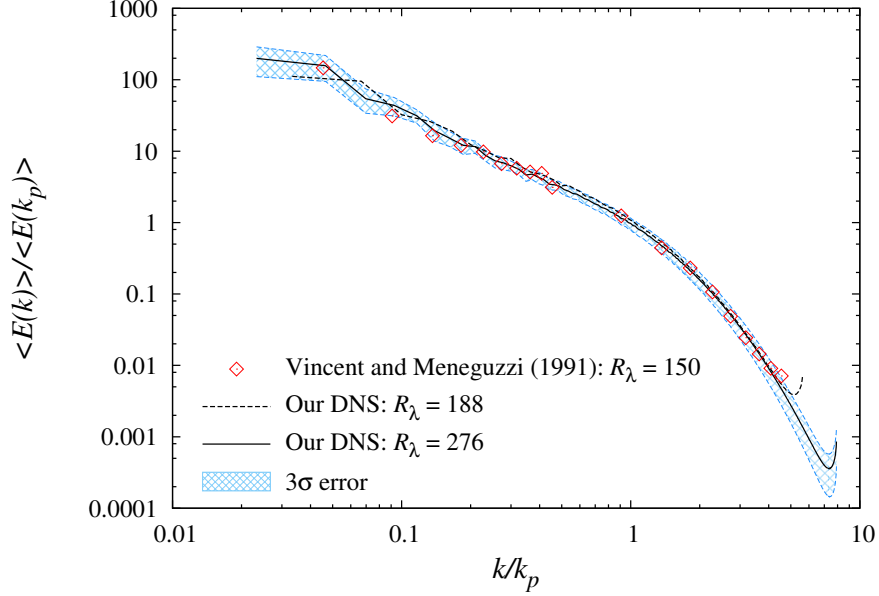


Figure 4: Comparison of dissipation-scaled energy spectra.

for which  $k_{\max}\eta > 1.5$ , see runs **f512c-g**. This allowed us to explore the distribution of energy and dissipation without artefacts caused due to the system being under-resolved. Figure 5 shows our results. We plot the total energy and dissipation rate which has been taken into account for up to mode  $k$  and normalised by their actual totals, thus

$$\frac{1}{\langle E \rangle} \int_{k_{\min}}^k dk' E(k') \quad \text{and} \quad \frac{1}{\langle \varepsilon \rangle} \int_{k_{\min}}^k dk' 2\nu_0 k'^2 E(k') . \quad (36)$$

We also plot the partially resolved run **f512b** for comparison, which can be seen to kick up unphysically as it reaches  $k\eta = 1$ . This also occurs for run **f512g** as it reaches its cutoff  $k_{\max}\eta = 1.7$ . The energy really is contained in much lower wavenumbers (larger length-scales) than the dissipative loss. By  $k\eta \sim 0.5$  we have already accounted for virtually all the energy, but only around 75% of the dissipation rate (see also [44]). The additional graphic in figure 5 shows a close up of the final percentile. This highlights two key points: First, if we want to include 99.5% of dissipative dynamics, we must use  $k_{\max}\eta \simeq 1.25$ . Whereas, to include 99.9% requires  $k_{\max}\eta \simeq 1.7$ . Second, as the Reynolds number is increased, energy is contained in progressively lower  $k\eta$  while dissipation is pushed to higher  $k\eta$ .

### 3.5 Isotropy

Since we wish to simulate isotropic turbulence, it is important to ensure that the velocity field does indeed satisfy this property. This was done using the method given in Young [55].

A random unit vector  $\mathbf{z}(\mathbf{k})$  which is not parallel to  $\mathbf{k}$  (that is, it satisfies  $\mathbf{z}(\mathbf{k}) \cdot \hat{\mathbf{k}} \neq 1$ ) is chosen for all wavevectors, and from it we define two mutually orthogonal unit vectors

$$\mathbf{e}_1(\mathbf{k}) = \frac{\mathbf{k} \times \mathbf{z}(\mathbf{k})}{|\mathbf{k} \times \mathbf{z}(\mathbf{k})|} , \quad \mathbf{e}_2(\mathbf{k}) = \frac{\mathbf{k} \times \mathbf{e}_1(\mathbf{k})}{|\mathbf{k} \times \mathbf{e}_1(\mathbf{k})|} . \quad (37)$$

These are used to compute the average energy in these two directions,

$$I_j(k, t) = \langle |\mathbf{e}_j(\mathbf{k}) \cdot \mathbf{u}(\mathbf{k}, t)|^2 \rangle , \quad j = 1, 2 , \quad (38)$$

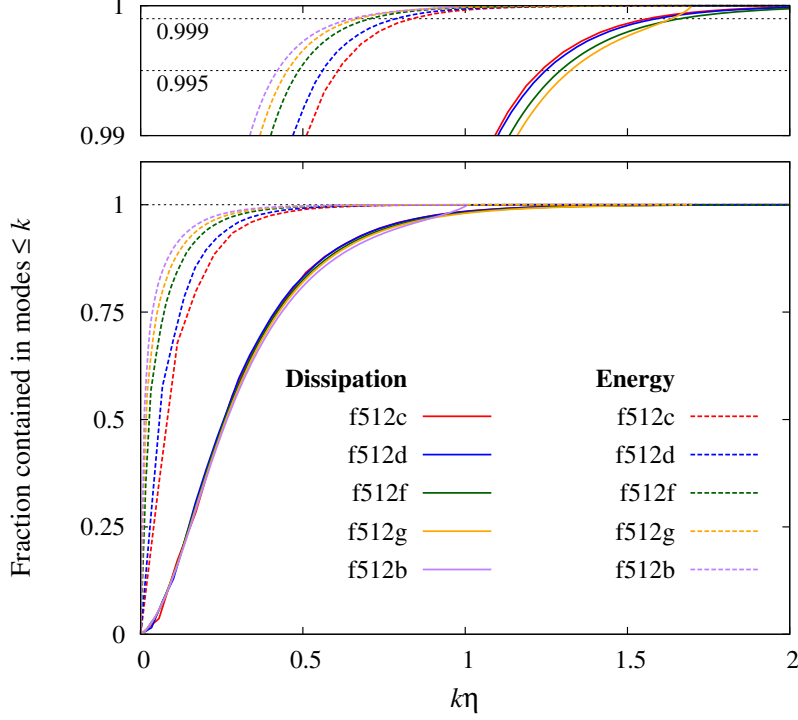


Figure 5: Location of energy and dissipation rate in highly resolved simulations. To retain 99.5% of dissipative dynamics, one must satisfy  $k_{\max}\eta > 1.25$  while 99.9% requires  $k_{\max}\eta > 1.7$ .

which should be the same for isotropic turbulence. A measure of the degree of isotropy is, therefore, the ratio

$$I(k, t) = \sqrt{\frac{I_1(k, t)}{I_2(k, t)}}. \quad (39)$$

As seen plotted in figure 6, while individual realisations fluctuate, the ensemble average is close to 1 for all values of  $k$ . The increase in the deviation from unity as one moves towards low  $k$  is due to the lower resolution of these shells. Since they contain fewer points the statistics are not as good.

A representative value can be obtained by averaging over all of Fourier space. Values for a variety of simulation sizes can be found in table 2 and are quite satisfactory, allowing us to conclude that there is no significant deviation from isotropy in our simulations. The uncertainty on the scale of the mean,  $\sigma/\langle I \rangle$ , decreases as  $N$  is increased, since the large  $k$  modes are more isotropic than the low  $k$  modes and we are including more of them in the simulation.

$N$	128	256	512	1024
$\langle I \rangle \pm \sigma$	$1.002 \pm 0.009$	$1.005 \pm 0.008$	$0.9979 \pm 0.0077$	$1.0002 \pm 0.0034$

Table 2: Representative values for the total isotropy for various lattice sizes.

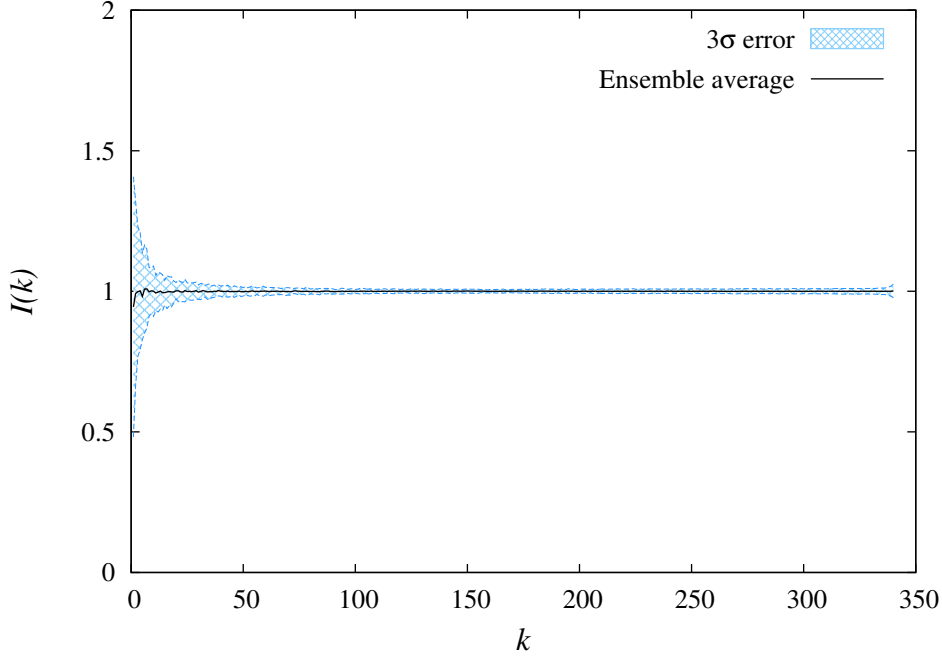


Figure 6: Ensemble averaged isotropy spectrum for an  $N = 1024$  lattice.

## 4 Results for scale-invariance and the Kolmogorov spectrum

The energy spectra taken for a selection of runs are presented in figure 7. Figure 7(a) is scaled using the Kolmogorov length-scale and the appropriate combination of dissipation range variables  $\varepsilon$  and  $\nu_0$ . The collapse of data for all runs is very good. The slope of the data can be seen to be slightly shallower than K41 for a period, hinting at  $-5/3 + \mu$  with  $\mu > 0$ . This is not in agreement with Kaneda, Ishihara and Yokokawa, Itakura and Uno [34] who found  $\mu \simeq -0.1$  by considering the compensated energy spectrum for the high Reynolds number simulations performed on the Earth Simulator. This correction could be Reynolds number dependent and vanish as  $Re \rightarrow \infty$ , making it a finite Reynolds number effect. An analysis of the Reynolds number variation of this exponent would help determine whether K41 is an asymptotic theory or not. Unfortunately, the data obtained here, presented in figure 7(c), did not offer a large enough range to measure this exponent properly. The compensated energy spectra should be compared to those obtained by Ishihara, Gotoh and Kaneda [46]. Figure 7(b) shows the energy spectrum scaled using the integral scale, for comparison. The slope here also looks to be shallower than  $k^{-5/3}$ .

The scaled transfer spectra are shown in figures 7(e) and 7(f).

### 4.1 The Kolmogorov prefactor

Figure 7(c) shows the compensated energy spectrum. Note the pronounced curl up of the tail for the partially resolved run **f512b**. This is also the case for **f1024b** (not plotted). The figure shows how a plateau could be identified for a low  $k\eta$  range for runs with  $R_\lambda > 113$ . This plateau was used to find a value for the Kolmogorov constant,  $\alpha$ , and can be seen to lie around 1.6 – 1.7. The values measured for the four runs for which a plateau could be found are given in table 3, using a simple average and an error-weighted fit. The transport power spectra shown in figure 7(d) were used to define the fit region. Note that the peak associated with  $k\eta \sim 0.1 - 0.2$  is

ID	$R_\lambda$	$\alpha$	$\alpha'$
f512a	176.9	$1.663 \pm 0.218$	$1.632 \pm 0.172$
f512b	203.7	$1.625 \pm 0.166$	$1.621 \pm 0.165$
f1024a	276.2	$1.636 \pm 0.177$	$1.646 \pm 0.144$
f1024b	335.2	$1.643 \pm 0.136$	$1.625 \pm 0.119$

Table 3: Measured values of the Kolmogorov constant, as found by identifying the range of wavenumbers where  $\Pi(k) \simeq \varepsilon$  and averaging over those points. The value  $\alpha$  is obtained by a simple average over the range, whereas  $\alpha'$  is calculated using an error-weighted fit on the range.

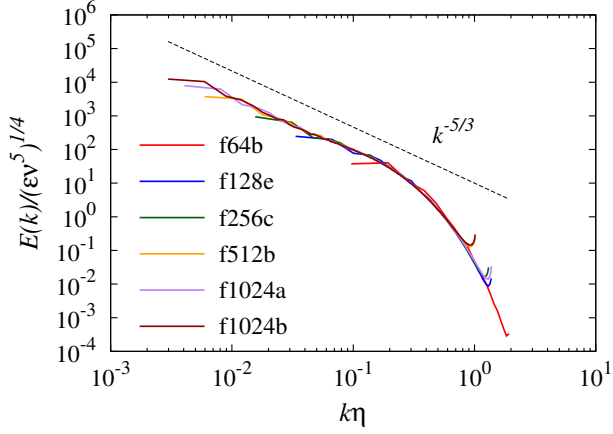
not associated with an inertial range. For runs with lower Reynolds number, a plateau cannot be identified.

## 4.2 Reynolds number dependence of statistics

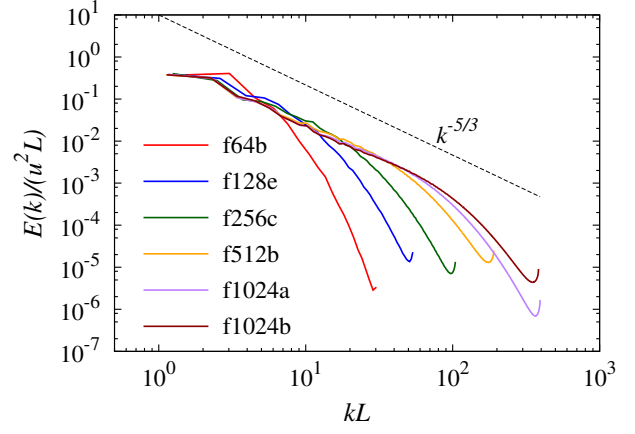
We now look at how the values of some important parameters vary with increasing Reynolds number. As mentioned in the previous section, an indication of the presence of a inertial subrange in a stationary system is a range of wavenumbers for which the transport power, or flux of energy through that wavenumber, is equal to the dissipation rate,  $\Pi(k) = \varepsilon$ . When this is the case, we find that the maximum transfer rate  $\varepsilon_T = \max \Pi(k) = \varepsilon$ . As such, a study of  $\varepsilon_T/\varepsilon$  will give unity for stationary systems in which the integral and dissipation scales are sufficiently well separated that an inertial subrange can form. The variation of this quantity with Reynolds number is presented in figure 8(a). This is in contrast to decaying turbulence, where the maximum transport can never quite reach the dissipation rate. Note that, for Reynolds numbers  $R_\lambda > 113$ , we basically find  $\varepsilon_T = \varepsilon$ , thus indicating the presence of an inertial subrange.

Figure 8(b) shows the Reynolds number variation of the steady state value of the rms velocity, integral and Taylor length-scales, and the velocity derivative skewness. We see that the skewness remains more or less constant, just above 0.5, for the range of Reynolds numbers available. The length-scales are both seen to decrease as  $Re$  increases. However, the integral scale looks like it may have reached a plateau, whereas the same cannot be said for the Taylor microscale. The rms velocity initially increases then appears to stay constant. We would expect the rms velocity to increase as the Reynolds number increases since there are more modes excited. This may still be the case, but as most of the energy is located at low wavenumbers the increase is small.

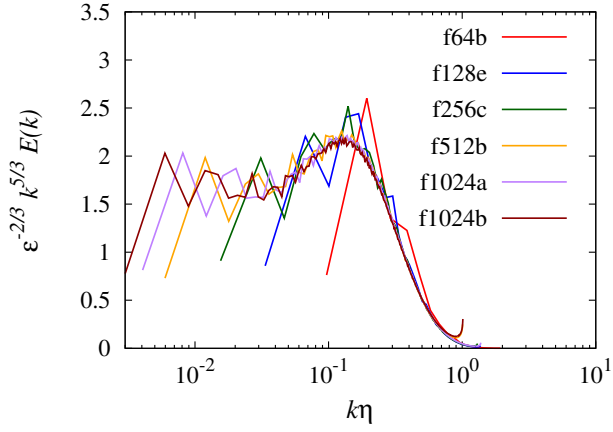
The Taylor surrogate  $u^3/L$  is compared in figure 8(c) to the dissipation rate and inertial flux,  $\varepsilon_T$ . We see that the surrogate is better matched to the behaviour of the inertial flux than the dissipation rate. This is in agreement with the findings of McComb *et al.* [56].



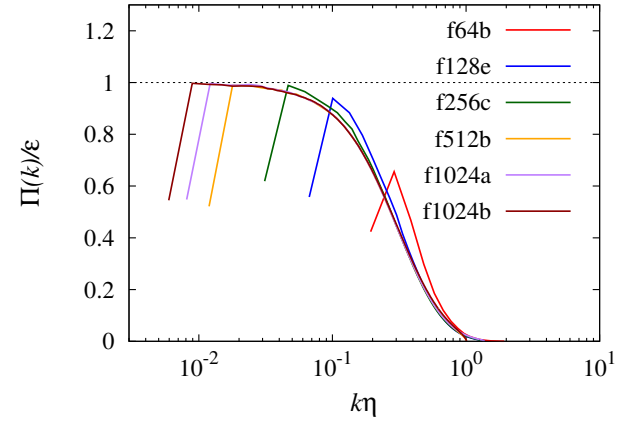
(a) Energy spectra scaled with  $\eta$



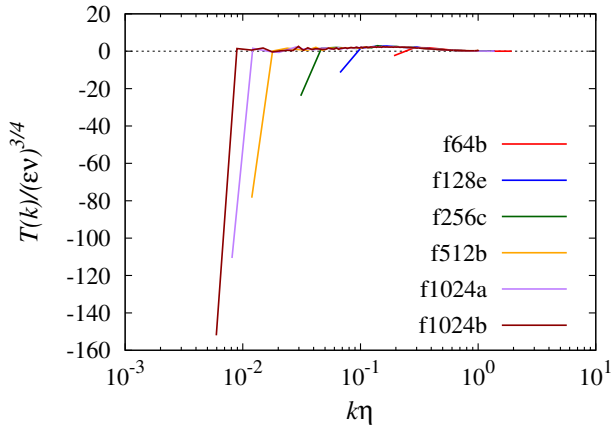
(b) Energy spectra scaled with the integral scale



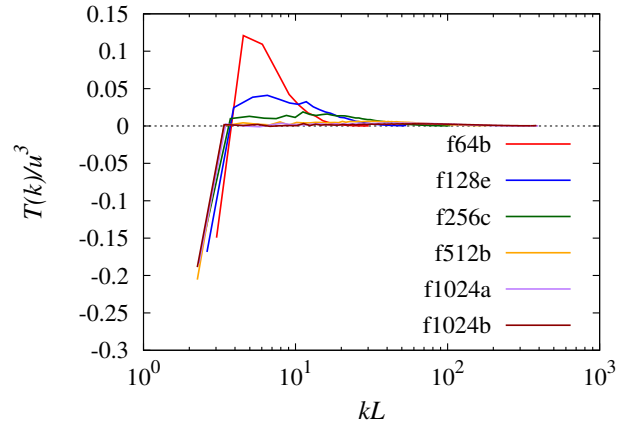
(c) The compensated energy spectrum



(d) The transport power spectrum



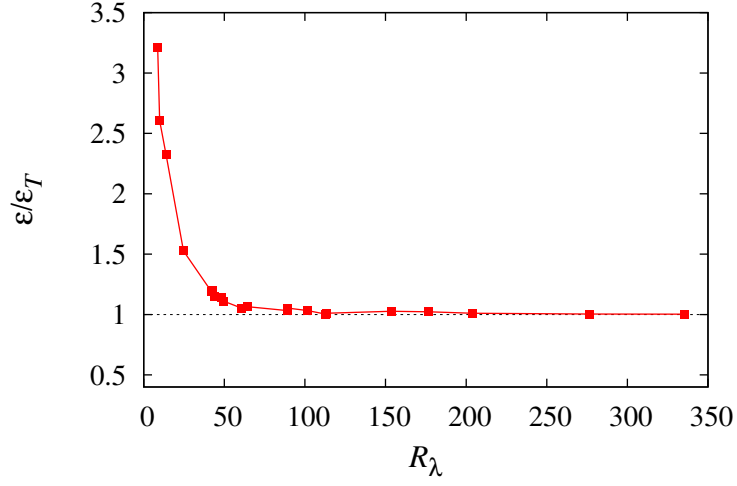
(e) Transfer spectra scaled with  $\eta$



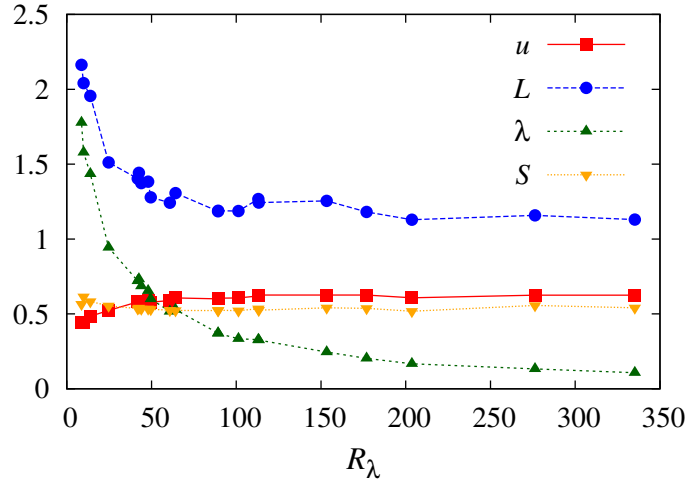
(f) Transfer spectra scaled with the integral scale

Figure 7: Energy, transfer and transport power spectra for the range of Reynolds numbers  $24.7 \leq R_\lambda \leq 335.2$ .

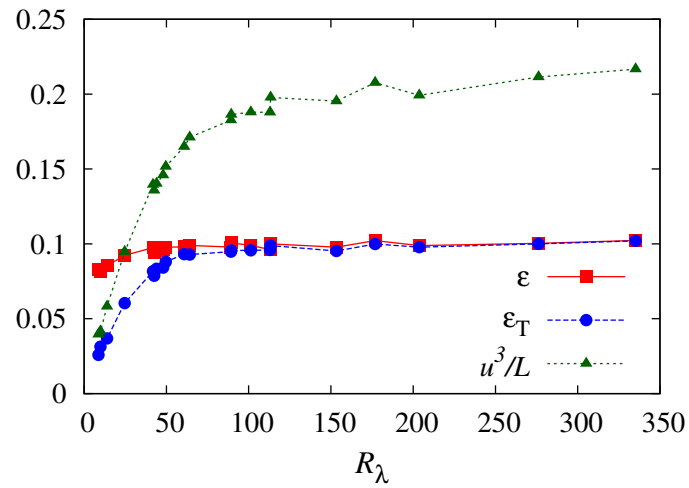




(a) Onset of an inertial subrange



(b) Variation of a selection of parameters



(c) The Taylor surrogate,  $u^3/L$

Figure 8: Variation of some key parameters with increasing Reynolds number.

## 5 Results illustrating the nature of internal intermittency

Internal intermittency was originally identified in terms of the drop-outs in an anemometer signal (see the monograph by Batchelor [57]). But it has long been interpreted as a spottiness in the spatial distribution of quantities like the vorticity or the rate-of-strain. In practice, this means that the phenomenon is seen as an example of a coherent structure. Thus, for many years it has been studied, in the context of coherent structures, by flow visualisation, in both laboratory experiments and numerical experiments (i.e. DNS). Of course in this topic there are many different criteria for establishing the presence of significant events, so we begin with some brief comments on flow-visualisation techniques. Then we discuss the ones that we have used here, before concluding with our results for the behaviour of the intermittency under ensemble-averaging.

### 5.1 Visualisation of coherent structures

Over the years, there have been many attempts to define a vortex in such a way that they may be identified in flow visualisation, whether that be experimental data from real flows or DNS data as studied here. The naïve definition of a vortex as a region of high vorticity can be misleading, since there is no particular value above which vorticity can be universally regarded as being high. In fact, even in the absence of vortices there can exist areas of high vorticity in parallel shear flows [58]. This creates a difficulty in finding unambiguous criteria which can isolate a unique vortex.

Jeong and Hussain [59] summarised and compared a selection of methods available. They highlighted that any criteria should be Galilean invariant, and found that previous indicators of a vortex, such as streamlines, isovorticity and minima in the local pressure are not suitable for use in unsteady flow. Haller [58] provided a comprehensive review of the definition of a vortex along with a variety of identification techniques. Despite this, surfaces of isovorticity continue to be used for vortex identification and can produce good results in the case of isotropic turbulence.

In this section, we will compare the detection of coherent structures in visualisations of our DNS data for isotropic turbulence using isovorticity contours, the  $Q$ -criterion, and the magnitude of the rate of strain.

#### 5.1.1 Isovorticity

Surfaces of isovorticity connect regions which have the same magnitude of vorticity,  $|\boldsymbol{\omega}|$ . Since the core of a vortex is associated with high vorticity, with the value progressively dropping as we move away from the core, these surfaces form structures such as ‘worms’ and ‘sheets’. See, for example, the work of Jimenez *et al.* [39] and Okamoto *et al.* [60]. From our results, structures identified in the plane  $z = 0$  using vorticity are shown in figures 9(a) and 10(b), for two different Reynolds numbers, as part of a comparison with other identification methods. As can be seen, the magnitude of vorticity shows a large amount of structure in the plane, and there are several regions of high vorticity that could be identified as being vortices. Three-dimensional structures can be seen in figures 11(a) and 13(a) and show how the vorticity has organised itself into an entanglement of tubes or ‘worms’, as observed by many other authors [46, 53, 39]. These should be compared to the Gaussian initial condition shown in figure 12(a), which shows little in the way of organised structure. Note that the plane with  $z = 0$  is through the centre of the box.

### 5.1.2 The $Q$ -criterion

The  $Q$ -criterion was originally proposed by Hunt, Wray and Moin [61] and is based on the invariants of the deformation tensor,  $A$ , whose elements are:

$$a_{ij} = \frac{\partial u_i}{\partial x_j} . \quad (40)$$

The eigenvalues,  $\Lambda$ , of this tensor are found by requiring that

$$\det(A - \Lambda \mathbb{I}) = 0 , \quad (41)$$

which in three-dimensions leads to the third-order characteristic equation,

$$\Lambda^3 - P\Lambda^2 + Q\Lambda - R = 0 , \quad (42)$$

with the coefficients:

$$P = \text{tr}(A); \quad (43)$$

$$Q = \frac{1}{2} \left( \text{tr}(A)^2 - \text{tr}(A^2) \right); \quad (44)$$

$$R = \det A . \quad (45)$$

The coefficients are the principle invariants of  $A$ , since the eigenvalues do not depend on the choice of basis vectors. We first note that:

$$\text{tr} A = \frac{\partial u_i}{\partial x_i} = 0, \quad (46)$$

for an incompressible fluid, such as that considered here. Next, the deformation tensor can be decomposed into its symmetric and antisymmetric parts, thus:

$$S_{ij} = \frac{1}{2} (a_{ij} + a_{ji}) \quad \text{and} \quad \Omega_{ij} = \frac{1}{2} (a_{ij} - a_{ji}) , \quad (47)$$

which may be recognised as the strain, and vorticity, tensors, respectively. We can therefore evaluate the trace

$$\begin{aligned} \text{tr}(A^2) &= \text{tr}(SS + S\Omega + \Omega S + \Omega\Omega), \\ &= \text{tr}(SS) + \text{tr}(S\Omega) + \text{tr}(\Omega S) + \text{tr}(\Omega\Omega), \\ &= \text{tr}(SS^T) - \text{tr}(S\Omega^T) + \text{tr}(\Omega S^T) - \text{tr}(\Omega\Omega^T) , \end{aligned} \quad (48)$$

where the last line used the symmetry of  $S$  and  $\Omega$ . Since the trace has the properties  $\text{tr}(AB) = \text{tr}(BA)$  and  $\text{tr}(A^T) = \text{tr}(A)$ , the two cross terms cancel, to leave:

$$Q = \frac{1}{2} \left( \|\Omega\|^2 - \|S\|^2 \right) , \quad (49)$$

with the Euclidean matrix norm defined as  $\|M\|^2 = \text{tr}(MM^T)$ . For the antisymmetric component, we have  $\|\Omega\|^2 = \frac{1}{2}|\boldsymbol{\omega}|^2$ , and the value of  $Q$  is calculated as

$$Q = \frac{1}{2} \left( \frac{1}{2}\omega^2 - \|S\|^2 \right) . \quad (50)$$

$Q$  represents the local balance between shear strain rate and vorticity magnitude, and vanishes at a solid boundary (unlike  $|\boldsymbol{\omega}|$ ) [59]. When  $Q > 0$ , the implication is that the vorticity

tensor (quantifying that amount of rotation) is dominant over the strain-rate tensor (which is related to dissipation), and so there is a vortex. Figure 9(c) shows the  $Q$ -criterion for a two-dimensional slice through a  $512^3$  evolved velocity field. As can be seen by comparison to 9(a) for the vorticity, the  $Q$ -criterion is more selective in what it considers to be coherent structures. Figures 11(c) and 13(b) show the three-dimensional structures identified using the  $Q$ -criterion. By comparison to those obtained using vorticity, we once again see that this method is stricter with what it considers to be a vortex. Note also that the ‘sheet’-like structures obtained using vorticity are no longer present. Comparison should be made to the Gaussian initial condition plotted in figure 12(b). See the work by Jeong and Hussain [59] and by Haller [58], and the many references therein, for more information and further discussion of these points.

### 5.1.3 Rate-of-strain

The rate-of-strain tensor  $S_{ij}$  defined above can be connected to the dissipation rate, since

$$\varepsilon = \frac{\nu_0}{2} \left\langle \left( \frac{\partial u_i}{\partial x_j} + \frac{\partial u_j}{\partial x_i} \right)^2 \right\rangle = 2\nu_0 \langle \|S\|^2 \rangle, \quad (51)$$

where the average is performed over space. This means that  $2\nu_0\|S\|^2$  gives a measure of the *local* dissipation at a point  $\mathbf{x}$ . Since  $2\nu_0$  is just a scaling, the magnitude of the strain rate tensor indicates the strength of the dissipation and allows for the identification of dissipative structures. We show these in figures 9(b) and 10(c): the former compares contours with the magnitude of vorticity and  $Q$ -criterion, discussed below, while the latter shows the structures for a higher Reynolds number on a larger lattice. Figure 11(b) shows the dissipative structures in three-dimensions, indicating that they are correlated with and attached to the regions of high vorticity, but that the two criteria are not indistinguishable.

## 5.2 Persistence of structure under averaging

Looking at the snapshot of the velocity field in figure (10a), it can be seen that there are well-defined structures and a great deal of variation from point to point. The velocity field is said to be intermittent: there is a high degree of spatial variation.

Due to the restriction of isotropy, it is impossible for coherent structure to exist in homogeneous, isotropic turbulence in anything other than an instantaneous sense [62]. To test the amount of residual coherent structure present in a finite ensemble, we ensemble average the velocity field. The set  $\mathbb{S}_N$  contains  $N$  realisations of the velocity field taken from a stationary simulation, sampled at an interval of one large eddy turnover time. The average is then found as

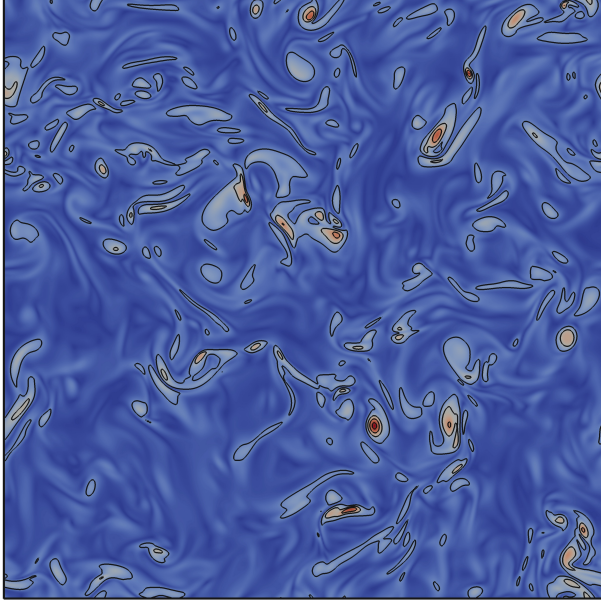
$$\langle \mathbf{u}(\mathbf{x}) \rangle_N = \frac{1}{N} \sum_{n=1}^N \mathbf{u}^{(n)}(\mathbf{x}), \quad (52)$$

where  $\mathbf{u}^{(n)}(\mathbf{x})$  is the  $n$ th member of  $\mathbb{S}_N$ . The resultant fields for a sample of  $N$  are visualised in figures 14 and 15 using vorticity and the  $Q$ -criterion, respectively. As can be seen in figure 14, the case  $N = 1$  corresponding to a single realisation displays the expected mass of structures. When we add in another realisation ( $N = 2$ ) we see a definite reduction in the amount of structure present; and this becomes even more dramatic when we move to  $N = 5$ . By this point, we have no structures with higher vorticity than our second lowest contour. Proceeding to  $N = 10$  and 25 the structures reduce further, until for  $N = 46$  we see only two very small areas with vorticity as high as 5% of  $\omega_{\max}$  obtained from the initial single realisation. A similar story is seen in figure 15 using the  $Q$ -criterion, with the difference that by  $N = 46$  there are

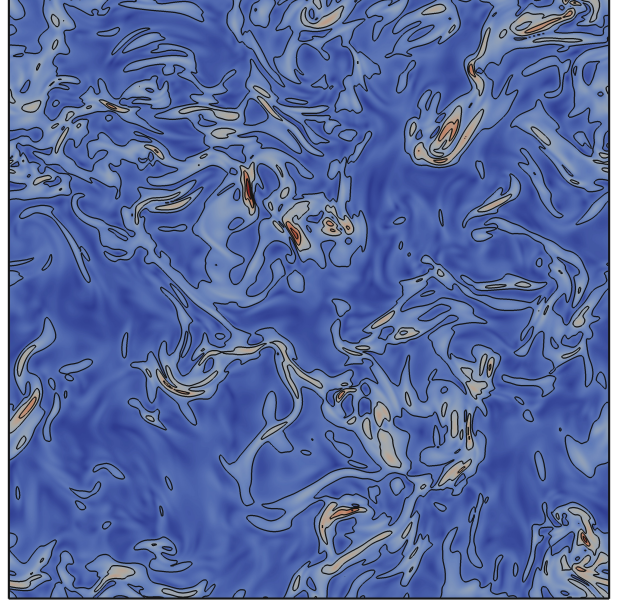
no structures present with even 0.5% of  $Q_{\max}$  obtained in  $N = 1$ . Note that there appear to be more structures in figure 15 than 9(c) above due to the inclusion of significantly lower, less restrictive contour values.

From this, we conclude that as the ensemble size is increased, there remains less and less coherent structure in the velocity field. The effect of intermittency, clearly present in a single realisation, on statistical quantities disappears as a result of ensemble averaging.

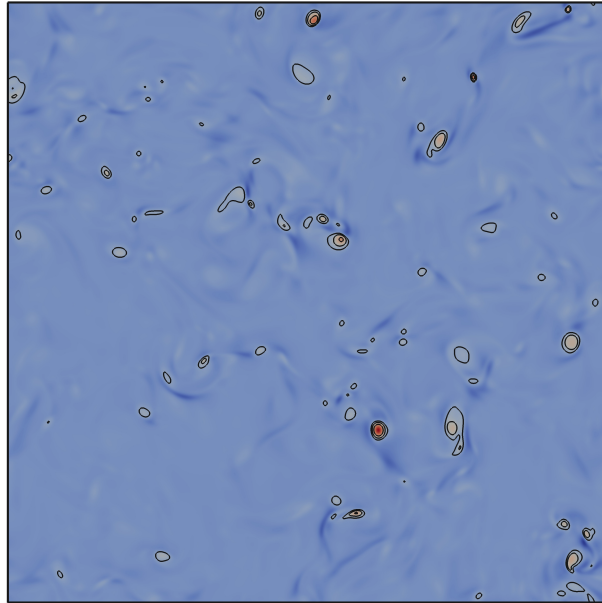
The constraint  $\langle \mathbf{u} \rangle = 0$  does not itself imply that there is no coherent structure which could remain under averaging, since one could set up, for example, two counter-rotating vortices. However, these structures break isotropy, and it is this which prevents their presence under the ensemble averaging process. This test therefore also assists in determining the degree to which isotropy is satisfied as the ensemble size is increased.



(a) Vorticity



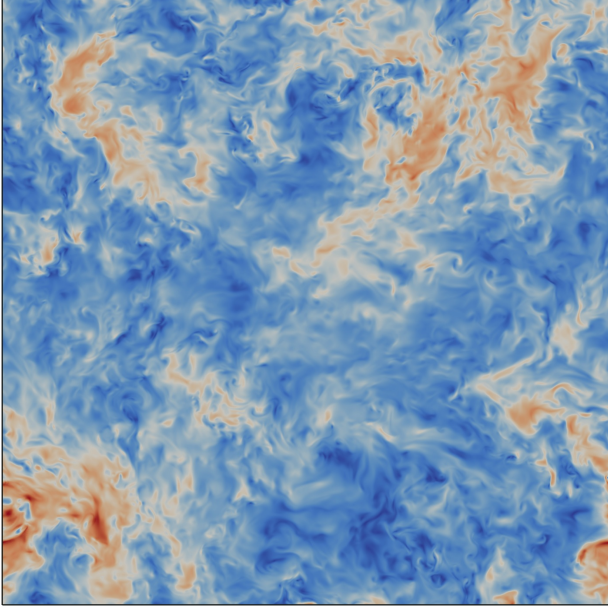
(b) Strain rate



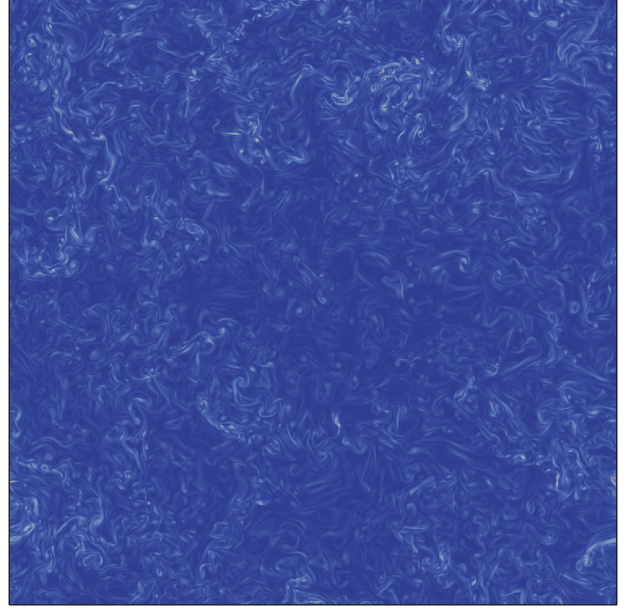
(c)  $Q$ -criterion

Figure 9: Visualisation of the  $z = 0$  plane of an  $R_\lambda \sim 115$  evolved velocity field from run **f512f**, using: (a) vorticity,  $|\boldsymbol{\omega}|$ ; (b) magnitude of the strain rate tensor,  $\|S\|$ ; and (c)  $Q$ -criterion. Contours for a range of values are also plotted. Note that the  $Q$ -criterion identifies far fewer structures. Contours for  $Q$ -criterion all have  $Q \geq 0.1Q_{\max}$ .

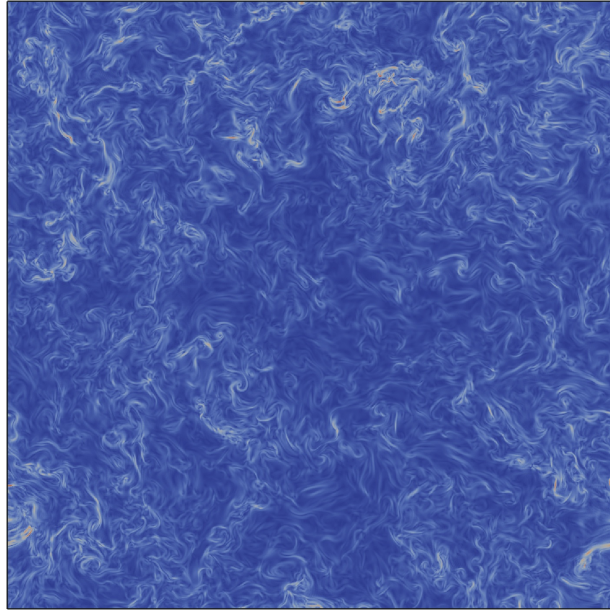




(a) Velocity

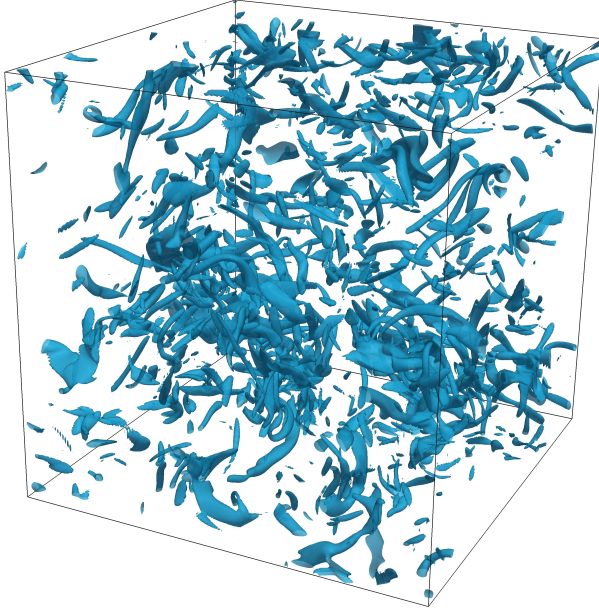


(b) Vorticity

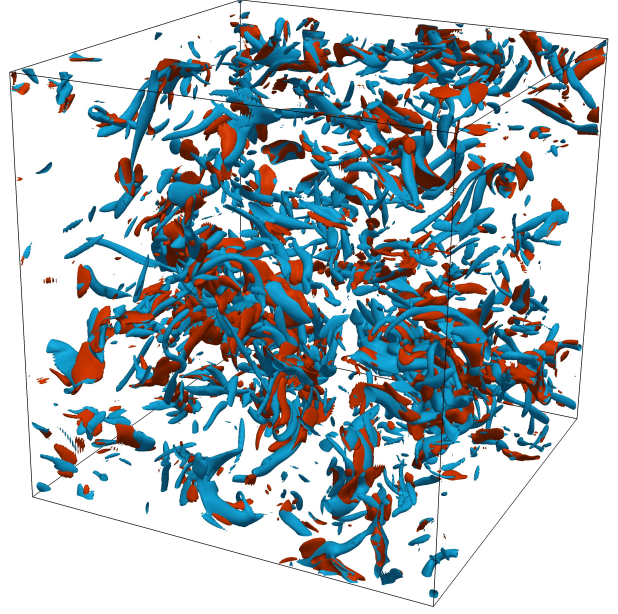


(c) Strain rate

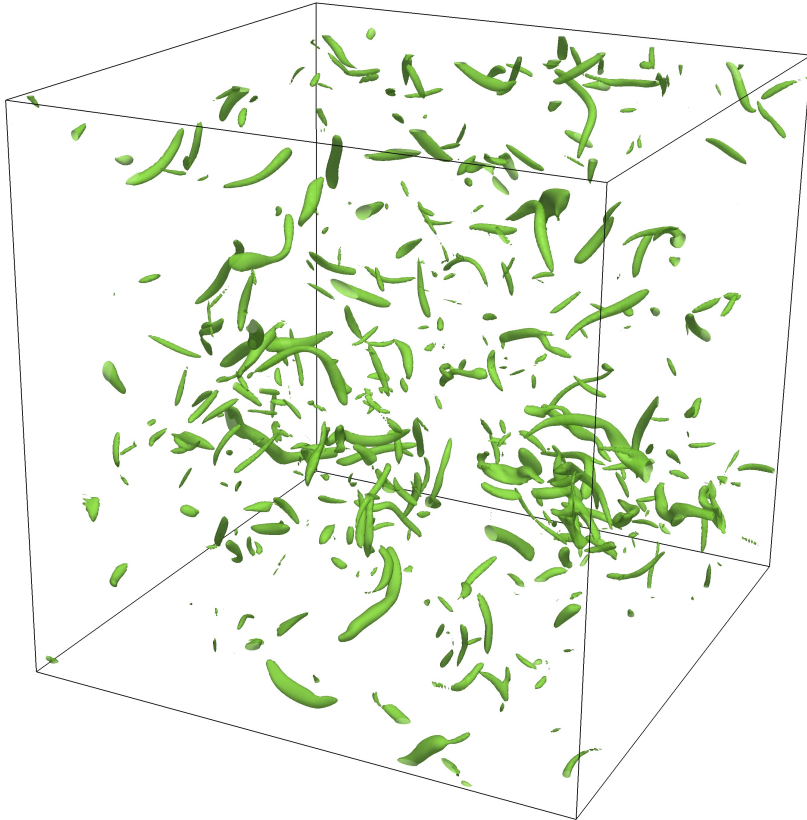
Figure 10: A snapshot of (the  $z = 0$  plane of) the evolved velocity field from run **f1024a**, coloured by: (a)  $|\mathbf{u}|$ ; (b)  $|\boldsymbol{\omega}|$ ; and (c) magnitude of the strain rate tensor,  $\|S\|$ . Contours not plotted due to the small size of the structures. Magnitude of velocity offers little in the way of identifying structures.



(a) Vorticity



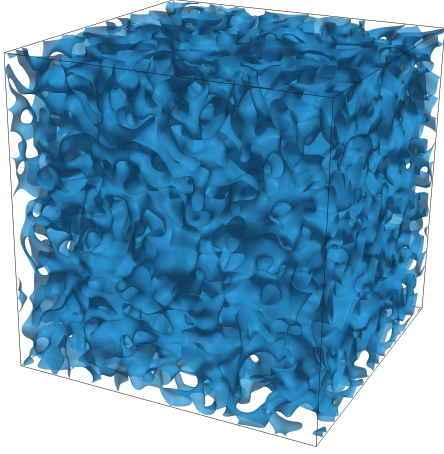
(b) Vorticity and rate-of-strain



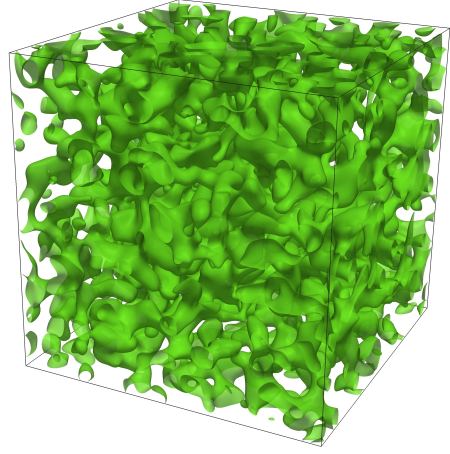
(c) Q-criterion

Figure 11: Visualisation of turbulent structures in an  $R_\lambda \sim 100$  evolved velocity field from run **f256b**. Isosurfaces of (a) vorticity ( $0.25\omega_{\max}$  plotted); (b) vorticity (blue) and strain rate ( $0.4\|S\|_{\max}$  plotted, red); and (c) Q-criterion ( $0.1Q_{\max}$  plotted). Regions of high vorticity are seen to be correlated with areas of high strain. The  $Q$ -criterion can be seen to pick out fewer structures than just vorticity.



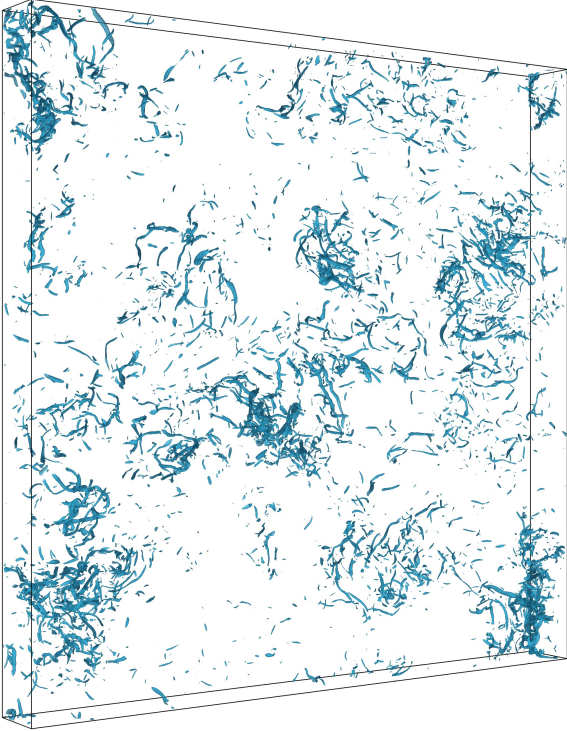


(a) Isovorticity

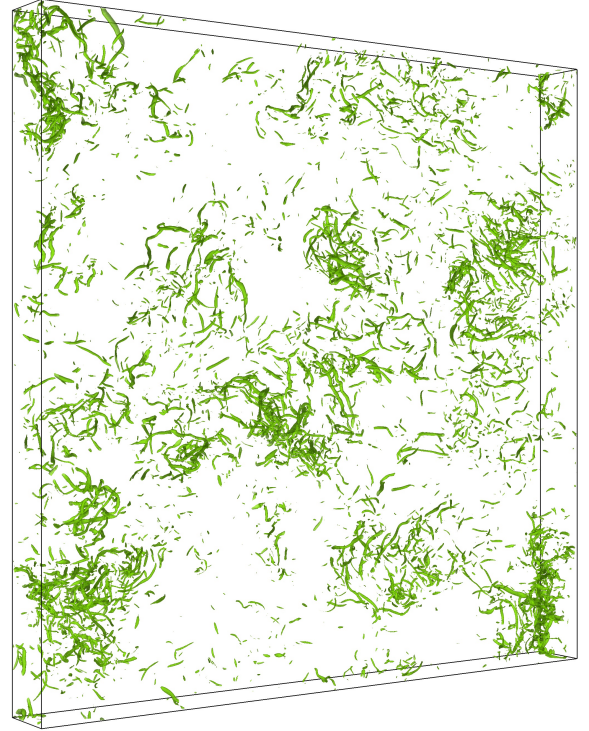


(b) Q-criterion

Figure 12: Visualisation of structures in an  $N = 256$  initial random Gaussian field. There is little evidence of coherent structure. The same surfaces have been plotted as figure 11 above.

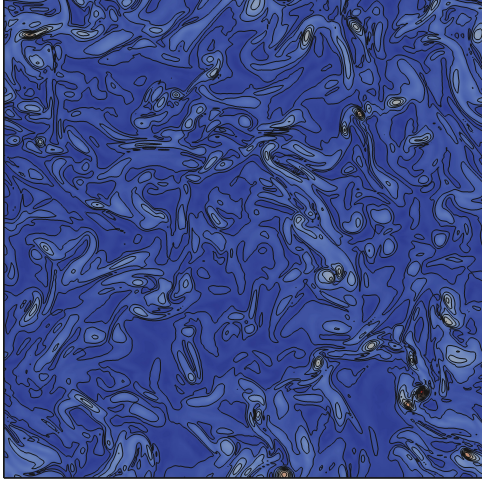


(a) Vorticity

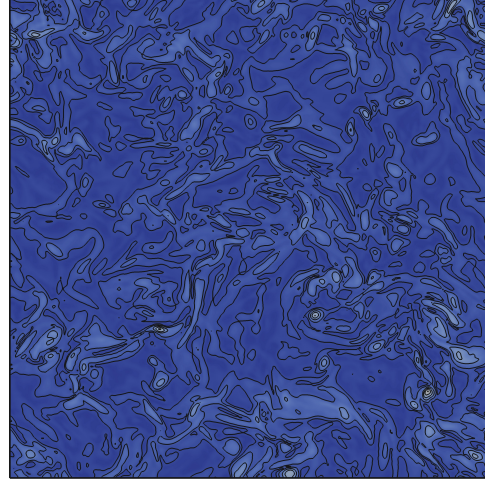


(b) Q-criterion

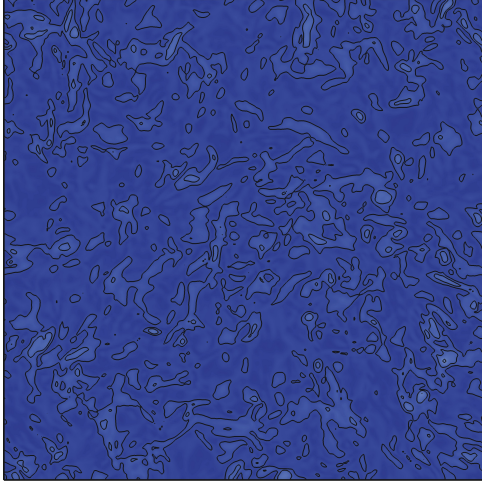
Figure 13: Visualisation of turbulent structures in a  $96 \times 1024 \times 1024$  slice (due to memory constraints, the whole volume could not be rendered) of an  $R_\lambda \sim 335$  evolved velocity field from run **f1024b**. Isosurfaces of (a) vorticity ( $0.25\omega_{\max}$  plotted) and (b) Q-criterion ( $0.05Q_{\max}$  plotted).



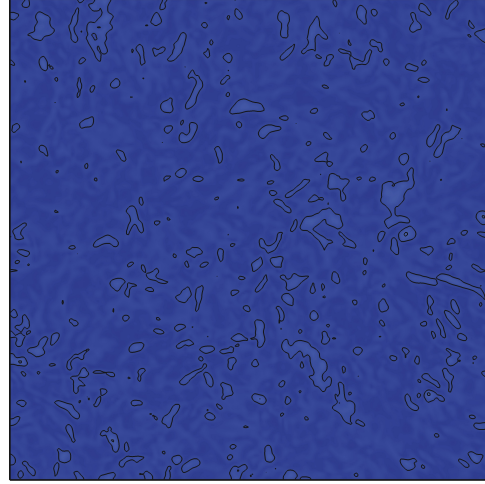
(a)  $N = 1$



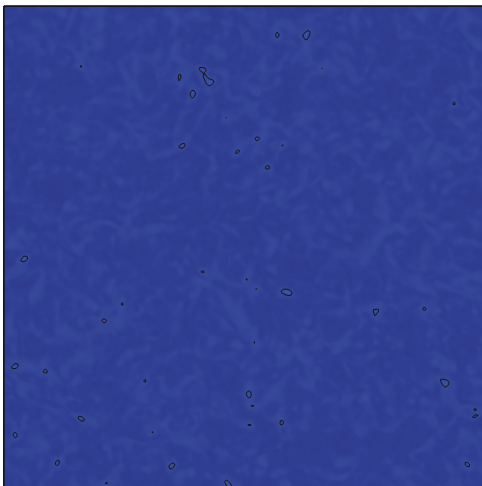
(b)  $N = 2$



(c)  $N = 5$



(d)  $N = 10$



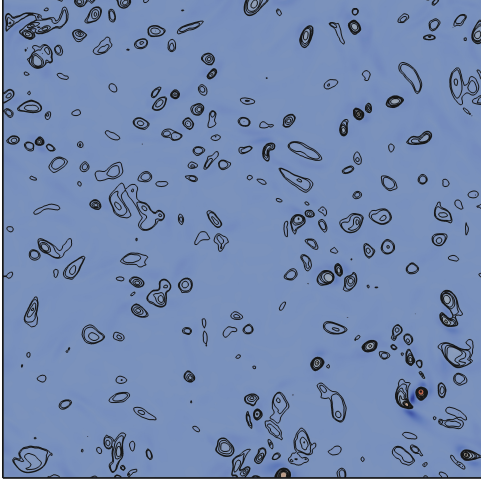
(e)  $N = 25$



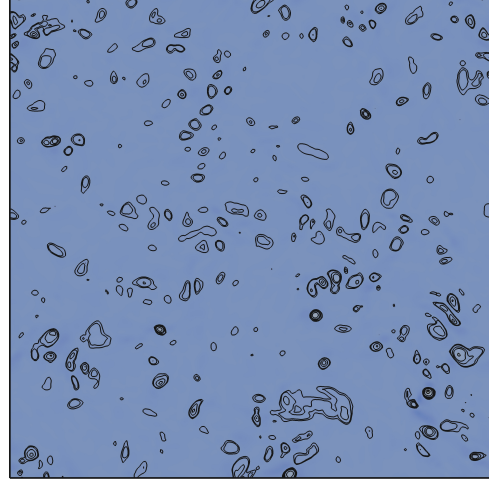
(f)  $N = 46$

Figure 14: Contours plotted for 5%, 10%, 20%, 30%, 40%, 50%, 60%, 70%, 80% and 90% of  $\omega_{\max}$ .  $R_\lambda \sim 100$  on  $256^3$  run f256b.

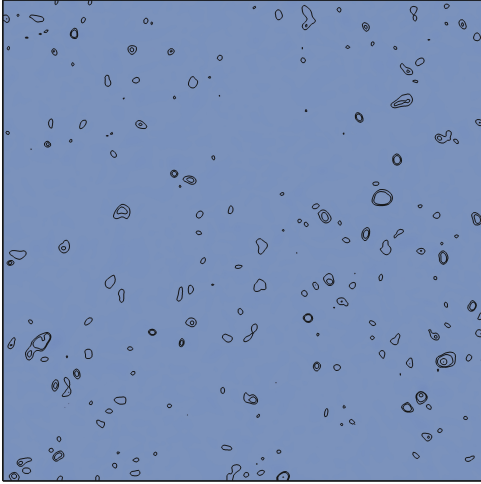




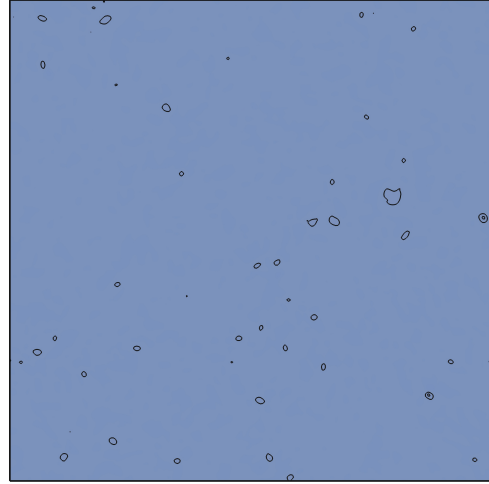
(a)  $N = 1$



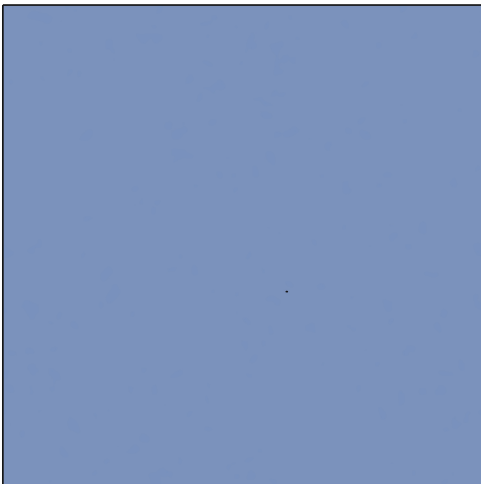
(b)  $N = 2$



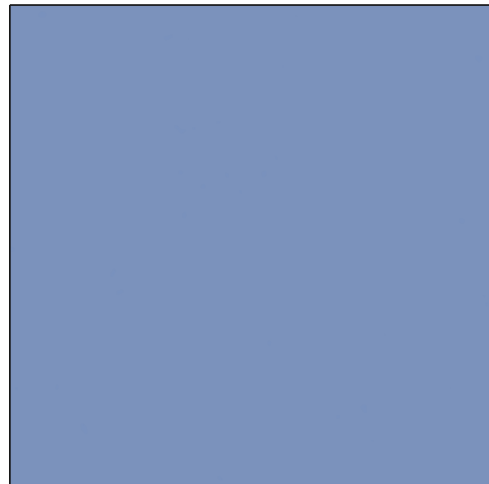
(c)  $N = 5$



(d)  $N = 10$



(e)  $N = 25$



(f)  $N = 46$

Figure 15: Contours plotted for 0.5%, 1%, 3%, 5%, 10%, 20%, 25%, 50%, 75% and 90% of  $Q_{\max}$ .  $R_\lambda \sim 100$  on  $256^3$  run f256b.

## 6 Discussion: intermittency effects *versus* finite-Reynolds-number corrections

In this section, we discuss various contentious issues concerning the Kolmogorov theory that have arisen over the years. These are: difficulties in reconciling the cascade picture with the physics of vortex stretching; the Landau criticism of K41; Kolmogorov's modified theory of 1962; anomalous exponents; and the more recent development of support for K41. We begin with a brief discussion of internal intermittency and highlight what we regard as the two most important points.

### 6.1 Internal intermittency

This type of intermittency was first pointed out by Batchelor and Townsend [63]. At one time, it was referred to as 'dissipation-range intermittency', and then more recently as 'fine-scale' or 'small-scale' intermittency. Nowadays it seems to be more usual to call it 'internal intermittency'. This is presumably because it is now recognized (mainly from numerical simulations) that this type of intermittency is present at all scales. In any case, it should be distinguished from the intermittency associated with a free edge of unconfined shear flows or with the 'bursting process' in duct flows. In both these cases, intermittency is associated with *structure*, which exists in some average sense. Due to its restrictive symmetries, it is impossible for structure to exist in isotropic turbulence, in anything other than an instantaneous sense.

There seem to be two crucial difficulties with the idea that the existence of spatial intermittency implies the need for some corrections to the Kolmogorov (1941) theory. These are as follows:

1. The dissipation rate is not the relevant quantity for K41A. The relevant quantity is the inertial flux of energy. The use of the same symbol  $\varepsilon$  (and even the same terminology!) for both these quantities may have caused some confusion. It is for this reason that we have introduced  $\varepsilon_T$  for flux (and also  $\varepsilon_D$  for decay rate) [14].
2. Internal intermittency is a phenomenon associated with a single realization. It must necessarily 'average out'; or, in other words, disappear, under any global averaging operation. It is not immediately obvious that its existence will affect relationships between globally-averaged quantities. In the case of K41B, Kolmogorov's starting point was the Kármán-Howarth equation and of course this equation is ensemble-averaged and contains the mean rate of dissipation. This fact was recognised in K62, where it was stated that the '4/5' law for  $S_3(r)$  was unaffected by the process of locally averaging the instantaneous dissipation rate  $\hat{\varepsilon}$  over a sphere of radius  $r$ . A significant new element in that work was the introduction of an *ad hoc* expression for the skewness and the abandonment of the assumption of constant skewness, as previously made in K41B.

However, despite the lack of any obvious connection between intermittency and the Kolmogorov theory, the use of the term 'intermittency effects' became quite widespread. By the 1980s, the exponent  $\mu$  was widely referred to as the *intermittency exponent*: see [64]. More recently the term *anomalous exponents* has become popular in connection with structure functions of all orders.

### 6.2 Cascade or vortex stretching?

The idea of a cascade, as believed to underpin the Kolmogorov picture, is often seen to be incompatible with the vortex-stretching behaviour of turbulence (e.g. see [65], [66]). In order

to examine this proposition, we need to understand the meaning of both these terms and indeed how they relate to the Kolmogorov theories.

The term ‘cascade’ is used to describe a process in which energy is transferred from large scales to small scales. However, there is no cascade in real space. This is because there is no inertial flux: the Kármán-Howarth equation is a *local* energy balance<sup>6</sup>, taken at a position  $\mathbf{x}$  or a scale  $r$ . Of course, in shear flows, the inhomogeneity leads to a flux of energy from where it is produced to where it is dissipated. But in isotropic turbulence no such flux exists. Good discussions of this topic may be found in the books by Tsinober [67] and that of Sagaut and Cambon [68] (who cite the first edition of Tsinober’s book).

How then does all this affect K41A and K41B, both of which were formulated in real space? Taking them in reverse order, K41B does not rely on a cascade. It relies on the vanishing of the viscous term in the Kármán-Howarth equation when one takes the limit of infinite Reynolds numbers at constant dissipation rate. Also, bearing in mind the local nature of the Kármán-Howarth equation, one may also apply a suitably chosen stirring force, such that its effects are confined to scales greater than some input scale  $r_I$ . Then the energy balance applies to an *inertial range of scales* where the detailed effects of dissipation and forcing are not felt. This separation of input (or energy-containing) scales from viscous dissipation scales offers a sort of intuitive basis for K41A, which is actually no more than a dimensional analysis.

It is generally understood that turbulence is characterised by various processes involving vortical structures, in which the vorticity increases with time in ways that we tend to associate with vortex stretching. One can think of a vortex tube being stretched by a velocity gradient, and in the process, conservation of angular momentum ensuring that the associated kinetic energy is concentrated in ever-smaller regions of space.

In the past, various models have been proposed to describe this process and these include arrays of tubes, plane vortex sheets, and so on. Naturally in each case, analytical tractability is a prime consideration in choosing the model. A brief introduction to such methods may be found in [64]. However, in recent years it has become clear, from numerical simulations of isotropic turbulence, that surfaces of constant vorticity tend to take the form of randomly-coiling worm-like structures.

When we seek to confront the cascade picture with the vortex-stretching picture, the difficulty in so doing is two-fold. First, the cascade is in wavenumber space, whereas the vortex structures are in real space. Second, the cascade is an ensemble-averaged process, whereas the vortex structure is an instantaneous phenomenon. It is characteristic of a single realization and may be eliminated by averaging. Nevertheless, it is still possible, in very general terms, to identify some apparent inconsistency between the two pictures, as follows.

Granted that the cascade describes the transfer of energy from small wavenumbers to large; and intuitively associating the corresponding ‘scales’ in  $x$ -space with the reciprocal of the wavenumbers, one can see a major difficulty in reconciling the two processes [65], [66]. That is, when a vortex tube is drawn out in space, the length scale of the extensional field may be expected to be much larger than the diameter of the extended tube. This is not immediately compatible with the idea of localness of a cascade. Or alternatively, when a vortex tube, or any comparable vortical structure, is stretched, at least one dimension of the structure remains large (when compared to the cross-section) and thus does not appear to support the idea of transfer to a larger wavenumber (i.e. smaller scales).

We can offer counter arguments to these points. But before doing so, let us enter a caveat. This to the effect that we should not rely too heavily on intuition about Fourier analysis, which

---

<sup>6</sup>This is not the case for the Navier-Stokes equation, where the pressure term is known to be non-local in real space [64]. But the NSE describes momentum transfer in a single realization, not ensemble-averaged energy transfer.

might just cope with Fourier transforms applied to some very simple problem such as waves in linear electric circuits or physical optics. In contrast, fluid turbulence is not only a highly nonlinear phenomenon but also involves random amplitudes and phases. In some many-body problems, the approximate cancellation of phases justifies a *random phase approximation*; and in other cases the phases are known to cancel exactly. Indeed, when we form the energy spectrum in turbulence, the phases cancel exactly by construction. But this does not alter the fact that making intuitive connections between phenomena in  $x$ -space and those in  $k$ -space is likely to prove a rather fraught procedure. Having said that, let us now take the two points in order.

The idea of localness is crucial to the cascade. When we consider the Fourier-transformed NSE, the first thing we learn is that nonlinear mixing couples each Fourier mode to every other mode. So it would be helpful if we had something like a ‘nearest neighbour’ assumption for interactions *e.g.* as in the Ising model for ferromagnetism). The situation is made worse in turbulence by the fact that the interactions between modes of the NSE are triadic. So the concept of ‘nearest neighbour’ is not available to us and has to be replaced by some idea of ‘strongly interacting triads’ and ‘weakly interacting triads’. This topic has been the subject of numerical investigations. For example, see the results of Domaradzki and Rogallo [69], Shanmugasundaram [70] and Yeung *et al.* [71]. The latter investigation is particularly interesting in our present context as it considers concurrent real-space and wavenumber-space views. However, interesting although these matters are, we do not need to rely on them in order to justify Kolmogorov’s picture. It was recognised by Batchelor [72], at least as early as the 1950s, that the key was not the transfer spectrum but the flux through mode  $k$ . This concept was implicit in the work of Obukhov [6] and Onsager [5]. It follows rigorously from the symmetry of the NSE, that the *local flux* through mode  $k$  is determined by a sum over all contributions  $j$  such that  $j \leq k$ . This, combined with scale invariance, is the only concept of localness that K41 needs. As the Reynolds number increases, and the energy-containing and dissipation ranges move apart, the inertial range becomes that range of wavenumbers where the flux is approximately constant and equal to the dissipation.

As regards the second point, one must be aware of identifying a vortical structure, such as a vortex tube, with a particular Fourier mode. If a given vortex tube contributes to  $u_1^2(k)$  and  $u_2^2(k)$ , where  $k$  is large; but not to the corresponding  $u_3^2(k)$ , then some other vortex tube (or, tubes) must make up the deficit. At the end of the day, the combined effects of ensemble-averaging and isotropy will ensure that this is so. We would reiterate that the Kolmogorov spectral picture involves only average quantities and reasoning from some speculation about a single realization is likely to prove tenuous at best.

### 6.3 The Landau criticism of K41 and problems with averages

The idea that K41 had some problem with the way that averages were taken has its origins in the famous footnote on page 126 of the book by Landau and Lifshitz [16]. This footnote is notoriously difficult to understand; not least because it is meaningless unless its discussion of the ‘dissipation rate  $\varepsilon$ ’ refers to the *instantaneous* dissipation rate. Yet  $\varepsilon$  is clearly defined in the text above (see the equation immediately before their (33.8)) as being the *mean* dissipation rate. Nevertheless, the footnote ends with the sentence ‘The result of the averaging therefore cannot be universal’. As their preceding discussion in the footnote makes clear, this lack of universality refers to ‘different flows’: presumably wakes, jets, duct flows, and so on.

We can attempt a degree of deconstruction as follows. We will use our own notation, and to this end we introduce the instantaneous structure function  $\hat{S}_2(r, t)$ , such that  $\langle \hat{S}_2(r, t) \rangle = S_2(r)$ . Landau and Lifshitz consider the possibility that  $S_2(r)$  could be a universal function in any

turbulent flow, for sufficiently small values of  $r$  (i.e. the Kolmogorov theory). They then reject this possibility, beginning with the statement:

‘The instantaneous value of  $\hat{S}(r, t)$  might in principle be expressed as a universal function of the energy dissipation  $\varepsilon$  at the instant considered.’

Now this is rather an odd statement. Ignoring the fact that the dissipation is not the relevant quantity for inertial-range behaviour, it is really quite meaningless to discuss the universality of a random variable in terms of its relation to a mean variable (i.e. the dissipation). A discussion of universality requires mean quantities. Otherwise it is impossible to test the assertion. The authors have possibly relied on their qualification ‘at the instant considered’. But how would one establish which instant that was for various different flows?

They then go on:

When we average these expressions, however, an important part will be played by the law of variation of  $\varepsilon$  over times of the order of the periods of the large eddies (of size  $\sim L$ ), and this law is different for different flows.’

This seems a rather dogmatic statement but, if  $\varepsilon$  is the *mean* dissipation rate, then it is clearly wrong for the broad (and important) class of stationary flows. In such flows, the mean dissipation rate  $\varepsilon$  does not vary with time.

Nevertheless, the authors conclude that: ‘The result of the averaging therefore cannot be universal.’

One has to make allowance for possible uncertainties arising in translation, but nevertheless, the latter argument only makes any sort of sense if the dissipation rate is also instantaneous. Such an assumption appears to have been made by Kraichnan [66], who provided an interpretation which does not actually depend on the *nature* of the averaging process. In fact Kraichnan worked with the energy spectrum, rather than the structure function, and interpreted Landau’s criticism of K41 as applying to

$$E(k) = \alpha \varepsilon^{2/3} k^{-5/3}. \quad (53)$$

His interpretation of Landau was that the prefactor  $\alpha$  may not be a universal constant because the left-hand side of equation (53) is, an average, while the right-hand side is the 2/3 power of an average. Any average involves the taking of a limit. Suppose we consider a time average, then we have

$$E(k) = \lim_{T \rightarrow \infty} \frac{1}{T} \int_0^T \hat{E}(k, t) dt, \quad (54)$$

where as usual the ‘hat’ denotes an instantaneous value. Clearly the statement

$$E(k) = \text{a constant}; \quad (55)$$

or equally the statement,

$$E(k) = f \equiv \langle \hat{f} \rangle, \quad (56)$$

for some suitable  $f$ , presents no problem. It is the ‘2/3’ power on the right-hand side of equation (53) which means that we are apparently equating the operation of taking a limit to the 2/3 power of taking a limit. However, it has recently been shown [14] that this issue is resolved by noting that the pre-factor  $\alpha$  itself involves an average over the phases of the system. It turns out that  $\alpha$  depends on an ensemble average to the  $-2/3$  power and this cancels the dependence on the 2/3 power on the right hand side of (53).

## 6.4 The Kolmogorov (1962) theory: a critical view

As we have already observed, Kolmogorov interpreted Landau's criticism as referring to the small-scale intermittency of the instantaneous dissipation rate. His response was to adopt Obukhov's proposal to introduce a dissipation rate which had been averaged over a sphere of radius  $r$ , which may be denoted by  $\varepsilon_r$ . This procedure runs into an immediate fundamental objection. In K41A, (or its wavenumber- space equivalent) the relevant inertial-range quantity for the dimensional analysis is the local (in wavenumber) energy transfer. Under certain circumstances, as is well known, this is equal to the mean dissipation rate by the global conservation of energy<sup>7</sup>. However, as pointed out by Kraichnan [66], there is no such simple relationship between locally-averaged energy transfer and locally-averaged dissipation.

Although Kolmogorov presented his 1962 theory as 'A refinement of previous hypotheses ...', following Kraichnan [66], it is now generally understood that this is incorrect. In fact it is a radical change of approach. The 1941 theory amounted to a general assumption that a cascade of many steps would lead to scales where the mean properties of turbulence were independent of the conditions of formation (i.e. of, essentially, the physical size of the system). Whereas, in 1962, the assumption was, in effect, that the mean properties of turbulence *did* depend on the physical size of the system. We will return to this point presently, but for the moment we concentrate on the preliminary steps.

The 1941 theory relied on a general assumption with an underlying physical plausibility. In contrast, the 1962 theory involved an arbitrary and specific assumption. This was to the effect that the logarithm of  $\varepsilon(\mathbf{x}, t)$  has a normal distribution for large  $L/r$  where  $L$  is referred to as an external scale and is related to the physical size of the system. We describe this as 'arbitrary' because no physical justification is offered; but in any case it is certainly specific. Then, arguments are developed that lead to a modified expression for the second-order structure function, thus:

$$S_2(r) = C(\mathbf{x}, t) \varepsilon^{2/3} r^{2/3} (L/r)^{-\mu}, \quad (57)$$

where  $C(\mathbf{x}, t)$  depends on the macrostructure of the flow.

In addition, Kolmogorov points out that 'the theorem of constancy of skewness ... derived (*sic*) in Kolmogorov (1941b)' is replaced by

$$S(r) = S_0 (L/r)^{3\mu/2}, \quad (58)$$

where  $S_0$  also depends on the macrostructure.

Equation (57) is rather clumsy in structure, in the way the prefactor  $C$  depends on  $x$ . This is because we have  $r = x - x'$ , so clearly  $C(\mathbf{x}, t)$  has an implicit dependence on  $r$ . A better way of tackling this would be to introduce centroid and relative coordinates,  $\mathbf{R}$  and  $\mathbf{r}$ , such that

$$\mathbf{R} = (\mathbf{x} + \mathbf{x}')/2; \quad \text{and} \quad \mathbf{r} = (\mathbf{x} - \mathbf{x}'). \quad (59)$$

Then we can re-write the prefactor as  $C(\mathbf{R}, r; t)$ , where the dependence on the macrostructure is represented by the centroid variable, while the dependence on the relative variable holds out the possibility that the prefactor becomes constant for sufficiently small values of  $r$ .

Of course, if we restrict our attention to homogeneous fields, then there can be no dependence of mean quantities on the centroid variable. Accordingly, one should make the replacement:

$$C(\mathbf{R}, r; t) = C(r; t), \quad (60)$$

---

<sup>7</sup>It is a potent source of confusion that these theories are almost always discussed in terms of dissipation  $\varepsilon$  when the proper inertial-range quantity is the nonlinear transfer of energy  $\Pi$ . The inertial range is defined by the condition  $\Pi_{max} = \varepsilon$



and the additional restriction to stationarity would eliminate the dependence on time. In fact Kraichnan [66] goes further and replaces the pre-factor with the constant  $C$ : see his equation (1.9).

For sake of completeness, another point worth mentioning at this stage is that the derivation of the ‘4/5’ law is completely unaffected by the ‘refinements’ of K62. This is really rather obvious. The Kármán-Howarth equation involves only ensemble-averaged quantities and the derivation of the ‘4/5’ law requires only the vanishing of the viscous term. This fact was noted by Kolmogorov [17].

Our final point under this heading has not, so far as we know, previously been made in the literature of the subject. That is, the energy spectrum is, in the sense of thermodynamics, an *intensive quantity*. Therefore it should not depend on the system size. This is, as opposed to the total kinetic energy (say) which does depend on the size of the system and is therefore *extensive*. What applies to the energy spectrum also applies to the second-order structure function. If we now consider equation (57), this contains the factor  $L^{-\mu}$ . Now,  $L$  is only specified as the external scale in K62, but it is necessarily related to the size of the system. Accordingly, taking the limit of infinite system size is related to taking the limit of infinite values of  $L$ , which is needed in order to have  $k = 0$  and to be able to carry out Fourier transforms. If we do this, we have three possible outcomes. If  $\mu$  is negative, then  $S_2 \rightarrow \infty$ , as  $L \rightarrow \infty$ , whereas if  $\mu$  is positive, then  $S_2$  vanishes in the limit of infinite system size. Hence, in either case, the result is unphysical, both by the standards of continuum mechanics and by those of statistical physics.

However, if  $\mu = 0$  then there is no problem. The structure function (and spectrum) exist in the limit of infinite system size. Could this be an argument for K41? At the end of this section, we will discuss a recent investigation which claims to be just that, and which may in some sense be related to the present point.

Lastly, we should mention that McComb and May [73] have used a plausible method to estimate values of  $L$  and, taking a representative value of  $\mu = 0.1$ , have shown that the inclusion of this factor (as in K62) destroys the well-known collapse of spectral data that can be achieved using K41 variables.

## 6.5 Anomalous exponents

The term *anomalous exponents* is used to refer to the case where the power-law exponents  $\zeta_n$  of structure functions  $S_n(r)$  differ from the Kolmogorov values  $n/3$ . The rise in interest in this topic has (unsurprisingly) gone hand in hand with the trend in recent years away from measurements of spectra to measurements of moments and structure functions in real space. Typically an experimental plot of exponents  $\zeta_n$  against  $n$  yields a curve in which the difference between  $\zeta_n$  and  $n/3$  increases with increasing  $n$ .

The idea of *anomalous exponents* seems to have arisen by analogy with the concept of *anomalous dimension* in the statistical field theory of equilibrium critical phenomena. However, such analogies should be interpreted with caution. In equilibrium, critical exponents determined by renormalization group methods differ from those obtained by dimensional analysis. The central role of the dimension of space in these theories leads to a natural interpretation in terms of anomalous dimension. But this situation arises because dimensional analysis is a very weak method in equilibrium problems and requires the introduction of densities in order to introduce dimensional considerations. In contrast, non-equilibrium systems are characterised by a symmetry-breaking current or flux. In the case of turbulence, this is the inertial transfer flux; and, combined with conservation of energy, this provides a strong constraint on dimensional analysis. A simple introduction to these ideas can be found in the book [74]. At the same time, it should be borne in mind that any systematic trend in the dependence of  $\zeta_n$  on  $n$ , with

increasing  $n$ , may be a systematic error due to the increasing importance of rare events with order  $n$ . This fact has been noted (although taken no further) by Frisch [75]. More recently, McComb *et al.* employed a standard technique from experimental physics to reduce the effects of systematic error and showed that the exponent of the second-order structure function tended to the Kolmogorov value of  $2/3$  as the Reynolds number tended to infinity.

The association of internal intermittency with anomalous exponents has developed strongly over the last few decades. Originally fractal models were popular (for an introductory discussion, see [64]) but later on multifractal models replaced them in popularity: for a recent review, see [76]. Over the same time, there has been a growing body of work supporting the obvious explanation for the deviation of exponents from the Kolmogorov (1941) values: namely that the conditions imposed by the theory are not fully satisfied at finite Reynolds numbers.

This disagreement is capable of being resolved. As direct numerical simulations increase in size and resolution, an examination of the dependence of  $\mu$  on Reynolds number should ultimately settle this question.

However we may conclude this part of our discussion with a salutary quotation, taken from Kraichnan's 1974 discussion of Kolmogorov's theories [66]. If  $E(k) \sim k^{-5/3+\mu}$  is asymptotically valid, then it follows that

'... the value of  $\mu$  depends on the details of the nonlinear interaction embodied in the Navier-Stokes equation and cannot be deduced from overall symmetries, invariance and dimensionality.'

In other words, perceived intermittency is an aspect of the solution of the Navier-Stokes equation.

## 6.6 Theoretical and experimental support for Kolmogorov (1941)

In addition to the extensive and indeed quite remarkable experimental support for the Kolmogorov spectrum, there are various investigations which, individually and collectively, offer considerable support to K41, rather than K62. Among the earliest in this category is the work by Effinger and Grossmann on the second-order structure function for the velocity field [77], which was later extended to structure functions of the temperature field in passive convection [78].

These authors studied the second-order structure function, by introducing a spatial smoothing operation in which they averaged the fluid velocity field  $u_\alpha(\mathbf{x}, t)$  over a sphere of radius  $r$ , thus:

$$u_\alpha^{(r)}(\mathbf{x}, t) = \langle u_\alpha(\mathbf{x}, t) \rangle^{(r)}, \quad (61)$$

where  $u_\alpha^{(r)}$  is referred to as the *super-scale* velocity field and the superscript on the angle-brackets indicates that the spatial average is taken over a sphere of radius  $r$ . The corresponding *sub-scale* velocity field  $\tilde{u}_\alpha^{(r)}$  was then obtained by subtraction, thus:

$$\tilde{u}_\alpha^{(r)}(\mathbf{x}, t) = u_\alpha(\mathbf{x}, t) - u_\alpha^{(r)}(\mathbf{x}, t). \quad (62)$$

The authors drew an analogy between their approach, and that of Reynolds, in which they operate on the NSE with (61) in order to derive separate equations of motion for the super-scale and sub-scale velocity fields. In principle, then, their strategy is to solve the equation for the sub-scale field and substitute the result into the equation for the super-scale field. In order to do this, they make a number of approximations, predominantly of the type used in renormalization group theory, which their method to some extent resembles. But, although approximate, their result for  $S_2$  agrees well with experimental results and its asymptotic behaviour supports K41 with viscous corrections.

As mentioned above, Effinger and Grossmann [78] extended this method to the problem of passive scalar convection. Later, this group presented an analysis of data from DNS which supported the idea that there are no intermittency corrections to energy spectra, when their results are extended to very high Reynolds numbers [79]; and more recently they have argued that the use of nonperturbative renormalization group methods enforces the K41 spectrum for isotropic turbulence [10].

Chronologically, our next approach is due to Qian, who has published a series of papers dealing with aspects of the scaling properties of isotropic turbulence; and, in particular, on deciding whether the second-order exponent  $\zeta_2$  corresponds to normal Kolmogorov scaling ( $\zeta_2 = 2/3$ ) or anomalous scaling ( $\zeta_2 > 2/3$ ). Here we shall concentrate on just three of these, that is [11], and the two papers leading up to it, [80, 81]. We may begin by noting that his method is different from all the other theoretical approaches, in that it is really a sophisticated form of data analysis, and is based on the use of exact relationships, combined with well-established data correlations, in order to extract as much information as possible from experimental results. Where assumptions are made, careful testing of the effect of varying these assumptions shows that they are innocuous.

We will give only a brief impression of this work and concentrate on his analysis of extended self-similarity or ESS. Qian shows that a log-log plot of  $S_2$  versus  $S_3$  produces the expected straight line. But when he plots the local gradient of that line against  $r/\eta$ , instead of being constant as one would expect, it shows a prominent peak, only becoming constant at large values of the scale. This in itself appears to question the validity of ESS. However, extending this work to higher-order structure functions, Qian demonstrates that the results from ESS actually support K41 rather than K62.

We cannot do justice to Qian's analysis here. The interested reader should consult the original papers which, although hard work, are rewarding. We now turn to the work of Barenblatt and Chorin, who also have published extensively on the theory of turbulence, particularly with reference to scaling and similarity, over a period of years. A good starting point is their two papers in 1988 [9, 82], which summarise their approach and which cite many earlier references. Their main emphasis is on the so-called 'law of the wall' in wall-bounded shear flows. However, they also deal with the inertial-range spectrum and conclude that the classical, unmodified K41 theory gives '... an adequate description of the local features of developed turbulent flows'. It is, of course, this latter aspect which concerns us here.

Essentially, Barenblatt and Chorin discuss the nature of scaling theory in turbulence. At the point where most people follow K62, and introduce the external length-scale to fill the gap in the dimensional analysis, these authors give arguments to support the use of the dissipation length-scale for this purpose. As a result they conclude that both the prefactor and the exponent in K41 are subject to corrections which are dependent on the Reynolds number. Overall, they conclude that '... there are no intermittency corrections to the Kolmogorov '5/3' spectral exponent'.

Next, we consider the first of two asymptotic matching theories: in this case for the energy spectrum. The work of Gamard and George [12] was motivated by the experimental study of Mydlarski and Warhaft [49], which reported finite Reynolds number effects in inertial-range spectra. As with other investigations discussed here, the paper cited is the outcome of a programme of work over some years and gives a number of references to previous work by George and co-workers.

Their starting point is the recognition that the energy spectrum can be scaled both on Kármán-Howarth variables (which gives a better collapse of data at low wavenumbers) and also on Kolmogorov variables (which gives a better collapse of data at high wavenumbers). Accordingly they introduced the dimensionless functions  $f_L$  for low wavenumbers, and  $f_H$  for

high wavenumbers. Recognising that  $f_L$  must asymptote to an inertial-range form for high wavenumbers and  $f_H$  must asymptote to an inertial-range form for low wavenumbers, Gamard and George set out to establish their functional form in a common region such that this form exists in the limit of infinite Reynolds numbers. Extension of this to finite Reynolds numbers involved some approximations, but these were checked by experimental comparisons at crucial stages. In a convincing analysis, they showed that the intermittency exponent  $\mu$  vanishes as the Reynolds number increases, in agreement with experiment.

Our second asymptotic analysis is the theory of Lundgren [13], who adopted a similar strategy to that of Gamard and George, but who worked in real space with the structure functions. Like them, he employed both Kármán-Howarth and Kolmogorov variables to scale the structure functions, and then matched asymptotic high-Reynolds expansions to obtain the Kolmogorov '2/3' law. However, where Gamard and George *demonstrate* the point, Lundgren *proves analytically* that the KH scaling (at large scales) and the Kolmogorov scaling (at small scales) are both asymptotically valid, as the Reynolds number tends to infinity. Matching asymptotic expansions, Lundgren concluded that, in the limit of infinite Reynolds numbers,  $S_2 \sim r^{2/3}$  and  $S_3 \sim r$ , in accordance with K41. In later work, Lundgren examined the dependence on Reynolds number in a more general way [83].

Gamard and George on the one hand, and Lundgren on the other, leave very little room for doubt. Their identical conclusions are to the effect that the predictions of K41 for  $E(k)$  or  $S_2(r)$  are subject to corrections due to finite viscosity and are asymptotically valid in the limit of infinite Reynolds number. Both can point to experimental support for their theoretical conclusions.

Returning to the spectral picture, we may make the observation that K41b relies on a *de facto* closure of the Kármán-Howarth equation as the viscosity tends to zero. The same idea can be employed in wavenumber space with the Lin equation [14], but here the effect of the phases can be taken into account explicitly. It transpires that the spectral prefactor arises from an integral over the phases and that the presence of this average resolves the problem of dependence on an average to the '2/3' power, as noted earlier. This work is related to the resolution of the inertial-range scale-invariance paradox [84] in 2008 (and more recently the introduction of a modified Lin equation which avoids the paradox [85]).

Turning now to approaches based on experiments (including numerical simulations) we have the investigations of Antonia and Burattini [86] in 2006 and Tchoufag, Sagaut and Cambon [87] in 2012. Both investigations found that the 4/5 law for  $S_3$  was approached asymptotically with increasing Reynolds number and that this approach was much slower in the case of decaying turbulence than for stationary turbulence. Antonia and Burattini cited Lindborg [88] for anticipating the difference between decaying and stationary isotropic turbulence; while Tchoufag *et al.* concluded that this difference was due to the non-negligible nature of the term  $\partial E(k, t)/\partial t$ . Note that McComb and Fairhurst [89] have used an asymptotic expansion in inverse powers of the Reynolds number to show that this term cannot be neglected by reason of restriction to certain scales nor to large Reynolds numbers. Also relevant, is the lack of a general criterion for the onset of turbulence in free decay, which to some extent hampers comparisons [21].

A much fuller treatment of the topics in this subsection may be found in Sections 6.4 and 6.5 of the book [18]. Here we mention the more recent investigations of Antonia, Djenidi and Tang [90, 91, 92, 93, 94], who have mounted a sustained attack on the problem of clarifying the relevance of the Kolmogorov theory. The last of these is a very remarkable paper which shows that applying Hölder's inequality to the exponents of the structure functions shows that the assumption  $\zeta_3 = 1$  leads to  $\zeta_2 = 2/3$ . It is tempting to conjecture that this may be relatable to Lundgren's analysis [13] and also to our present use of realizability criteria at the end of subsection 6.4 of the present work.

## 7 Conclusion

It is difficult to avoid concluding that much of the confusion over intermittency corrections arises from the fact that, as we have discussed, K41A is not a completely satisfactory theory. There is no cascade in real space and the dimensional analysis seems to rely on some sort of intuitive appeal to what is going on behind the scenes, as it were, in wavenumber space. There we have the concept of flux of energy from *all* lower wavenumbers to the wavenumber of interest. This is due to an exact symmetry of the equations of motion. The necessary additional concept of scale invariance (which defines the inertial range) arises inevitably as the Reynolds number increases and the dissipation is pushed to ever-higher wavenumbers. This also is a property of the NSE. Perhaps, in principle, it would be better to first carry out the analysis in wavenumber space and then recover the inertial-range form of  $S_2(r)$  by Fourier transformation? In any case, we have argued here for the combination of the two approaches into the Kolmogorov-Obukhov theory, as indeed was sometimes done many years ago.

In contrast, K41B, as a prediction of the inertial-range form of the third-order structure function, is incontrovertible. The analysis is asymptotically exact for stationary turbulence and the Kolmogorov form must apply at infinite Reynolds numbers. From this, two points arise as a corollary. They are, as follows:

1. Any theory or procedure which relies on the assumption that the scaling exponent of  $S_3$  is exactly  $n = 1$  at finite Reynolds numbers is already subject to error, however small.
2. The fact that  $S_3$  is subject to finite-viscosity corrections sets a precedent for  $S_2$  which is rigorously connected to it by conservation of energy.

Overall, our numerical results, in agreement with those from other investigations, support the Obukhov picture of the onset of scale-invariance of the inertial flux of energy to higher wavenumbers and the inevitable consequence that the energy spectrum is given by the ‘5/3’ law. The disappearance of the intermittency under ensemble-averaging is a necessary consequence of the isotropy and for those who understand that, this is a reassuring test of the isotropy of our statistical ensemble. For those who do not, it is a demonstration that the internal intermittency has no consequences for the inertial-range flux and hence no consequences for the Kolmogorov-Obukhov theory.

Essentially, we have re-phrased the question about intermittency effects on the energy spectrum. Instead of asking: does intermittency alter the 5/3 exponent, we have asked: does intermittency affect the onset of scale-invariance of the energy flux? And the answer seems to be that it cannot! However, it should be borne in mind that our present discussion is limited to stationary, homogeneous, isotropic turbulence and our conclusions may have to be modified for any more general situation. The necessity for this type of examination for other classes of flow must be borne in mind.

## Acknowledgement

*Simulations were performed on the Eddie HPC cluster hosted by the Edinburgh Parallel Computing Centre (EPCC). Data are available online [<http://dx.doi.org/10.15129/64a4a042-7d0d-48ce-8afa-21f9883d1e84>].*

Website for hit3d: <http://code.google.com/p/hit3d/>

## References

- [1] J. L. Lumley and A. M. Yaglom. A Century of Turbulence. *Flow, Turbulence and Combustion*, 66:241, 2001.
- [2] A. N. Kolmogorov. The local structure of turbulence in incompressible viscous fluid for very large Reynolds numbers. *C. R. Acad. Sci. URSS*, 30:301, 1941.
- [3] L. F. Richardson. *Weather Prediction by Numerical Process*. Cambridge University Press, 1963.
- [4] G. K. Batchelor. Kolmogorov’s theory of locally isotropic turbulence. *Proc. Camb. Philos. Soc.*, 43:533, 1947.
- [5] L. Onsager. The Distribution of Energy in Turbulence. *Phys. Rev.*, 68:281, 1945.
- [6] A. M. Obukhov. On the distribution of energy in the spectrum of turbulent flow. *C.R. Acad. Sci. U.R.S.S.*, 32:19, 1941.
- [7] F. Anselmet, Y. Gagne, E. J. Hopfinger, and R. A. Antonia. High-order velocity structure functions in turbulent shear flows. *J. Fluid Mech.*, 140:63, 1984.
- [8] John C. Bowman. On inertial-range scaling laws. *J. Fluid Mech.*, 306:167–181, 1996.
- [9] G. I. Barenblatt and A. J. Chorin. New perspectives in turbulence: scaling laws, asymptotics and intermittency. *SIAM Rev.*, 40:265–291, 1998.
- [10] A. Esser and S. Grossmann. Nonperturbative renormalisation group approach to turbulence. *Eur. Phys. J. B*, 7:467–482, 1999.
- [11] J. Qian. Closure Approach to High-Order Structure Functions of Turbulence. *Physical Review Letters*, 84(4):646–649, 2000.
- [12] S. Gamard and W. K. George. Reynolds number dependence of energy spectra in the overlap region of isotropic turbulence. *Flow, turbulence and combustion*, 63:443–477, 1999.
- [13] Thomas S. Lundgren. Kolmogorov two-thirds law by matched asymptotic expansion. *Phys. Fluids*, 14:638, 2002.
- [14] David McComb. Scale-invariance and the inertial-range spectrum in three-dimensional stationary, isotropic turbulence. *J. Phys. A: Math. Theor.*, 42:125501, 2009.
- [15] A. N. Kolmogorov. Dissipation of energy in locally isotropic turbulence. *C. R. Acad. Sci. URSS*, 32:16, 1941.
- [16] L. D. Landau and E. M. Lifshitz. *Fluid Mechanics*. Pergamon Press, London, English edition, 1959.
- [17] A. N. Kolmogorov. A refinement of previous hypotheses concerning the local structure of turbulence in a viscous incompressible fluid at high Reynolds number. *J. Fluid Mech.*, 13:82–85, 1962.
- [18] W. David McComb. *Homogeneous, Isotropic Turbulence: Phenomenology, Renormalization and Statistical Closures*. Oxford University Press, 2014.

- [19] W. D. McComb. Infrared properties of the energy spectrum in freely decaying isotropic turbulence. *Phys. Rev. E*, 93:013103, 2016.
- [20] W. David McComb, Arjun Berera, Matthew Salewski, and Sam R. Yoffe. Taylor’s (1935) dissipation surrogate reinterpreted. *Phys. Fluids*, 22:61704, 2010.
- [21] S. R. Yoffe and W. D. McComb. Onset criteria for freely decaying turbulence. *Phys. Rev. Fluids*, 3:104605, 2018.
- [22] W. D. McComb, S. R. Yoffe, M. F. Linkmann, and A. Berera. Spectral analysis of structure functions and their scaling exponents in forced isotropic turbulence. *Phys. Rev. E*, 90:053010, 2014.
- [23] W. D. McComb, A. Berera, S. R. Yoffe, and M. F. Linkmann. Energy transfer and dissipation in forced isotropic turbulence. *Phys. Rev. E*, 91:043013, 2015.
- [24] W. D. McComb, M. F. Linkmann, A. Berera, S. R. Yoffe, and B. Jankauskas. Self-organization and transition to turbulence in isotropic fluid motion driven by negative damping at low wavenumbers. *J. Phys. A Math.Theor.*, 48:25FT01, 2015.
- [25] A. Berera and M. Linkmann. Magnetic helicity and the evolution of decaying magnetohydrodynamic turbulence. *Phys. Rev. E*, 90:013007–1–25, 2014.
- [26] M. F. Linkmann, A. Berera, W. D. McComb, and M. E. McKay. Nonuniversality and Finite Dissipation in Decaying Magnetohydrodynamic Turbulence. *Phys. Rev. Lett.*, 114:235001, 2015.
- [27] S. R. Yoffe. *Investigation of the transfer and dissipation of energy in isotropic turbulence*. PhD thesis, University of Edinburgh, 2012.
- [28] S. G. Chumakov. Scaling properties of subgrid-scale energy dissipation. *Phys. Fluids*, 19:058104, 2007.
- [29] S. G. Chumakov. A priori study of subgrid-scale flux of a passive scalar in turbulence. *Phys. Rev. E*, 78:15563, 2008.
- [30] M. E. Brachet, D. I. Meiron, S. A. Orszag, B. G. Nickel, R. H. Morf, and U. Frisch. Small-scale structure of the Taylor-Green vortex. *J. Fluid Mech.*, 130:411–452, 1983.
- [31] L.-P. Wang, S. Chen, J. G. Brasseur, and J. C. Wyngaard. Examination of hypotheses in the Kolmogorov refined turbulence theory through high-resolution simulations. Part 1. Velocity field. *J. Fluid Mech.*, 309:113, 1996.
- [32] N. Cao, S. Chen, and G. D. Doolen. Statistics and structures of pressure in isotropic turbulence. *Phys. Fluids*, 11:2235–2250, 1999.
- [33] T. Gotoh, D. Fukayama, and T. Nakano. Velocity field statistics in homogeneous steady turbulence obtained using a high-resolution direct numerical simulation. *Phys. Fluids*, 14:1065, 2002.
- [34] Y. Kaneda, T. Ishihara, M. Yokokawa, K. Itakura, and A. Uno. Energy dissipation and energy spectrum in high resolution direct numerical simulations of turbulence in a periodic box. *Phys. Fluids*, 15:L21, 2003.

- [35] D. A. Donzis, K. R. Sreenivasan, and P. K. Yeung. Scalar dissipation rate and dissipative anomaly in isotropic turbulence. *J. Fluid Mech.*, 532:199–216, 2005.
- [36] P. K. Yeung, D. A. Donzis, and K. R. Sreenivasan. Dissipation, enstrophy and pressure statistics in turbulence simulations at high Reynolds numbers. *J. Fluid Mech.*, 700:5–15, 2012.
- [37] S. A. Orszag. On the Elimination of Aliasing in Finite-Difference Schemes by Filtering High-Wavenumber Components. *J. Atmos. Sc.*, 28:1074, 1971.
- [38] K. Heun. Neue Methoden zur approximativen Integration der Differentialgleichungen einer unabhängigen Veränderlichen. *Z. Math. Phys.*, 45:23–38, 1900.
- [39] J. Jiménez, A. A. Wray, P. G. Saffman, and R. S. Rogallo. The structure of intense vorticity in isotropic turbulence. *J. Fluid Mech.*, 255:65, 1993.
- [40] L. Machiels. Predictability of small-scale motion in isotropic fluid turbulence. *Phys. Rev. Lett.*, 79(18):3411–3414, 1997.
- [41] Y. Yamazaki, T. Ishihara, and Y. Kaneda. Effects of Wavenumber Truncation on High-Resolution Direct Numerical Simulation of Turbulence. *J. Phys. Soc. Jap.*, 71:777–781, 2002.
- [42] Y. Kaneda and T. Ishihara. High-resolution direct numerical simulation of turbulence. *Journal of Turbulence*, 7:1–17, 2006.
- [43] Charles R. Doering and Nikola P. Petrov. Low-wavenumber forcing and turbulent energy dissipation. *Progress in Turbulence*, 101(1):11–18, 2005.
- [44] W. D. McComb, A. Hunter, and C. Johnston. Conditional mode-elimination and the subgrid-modelling problem for isotropic turbulence. *Phys. Fluids*, 13:2030, 2001.
- [45] P. K. Yeung and Y. Zhou. Universality of the Kolmogorov constant in numerical simulations of turbulence. *Phys. Rev. E*, 56:1746, 1997.
- [46] T. Ishihara, T. Gotoh, and Y. Kaneda. Study of high-Reynolds number isotropic turbulence by direct numerical simulation. *Ann. Rev. Fluid Mech.*, 41:165, 2009.
- [47] T. Gotoh and D. Fukayama. Pressure spectrum in homogeneous turbulence. *Phys. Rev. Lett.*, 86:3775, 2001.
- [48] K. R. Sreenivasan. On the universality of the Kolmogorov constant. *Phys. Fluids*, 7:2778, 1995.
- [49] L. Mydlarski and Z. Warhaft. On the onset of high-Reynolds-number grid-generated wind tunnel turbulence. *J. Fluid Mech.*, 320:331–368, 1996.
- [50] A. Vincent and M. Meneguzzi. The spatial structure and statistical properties of homogeneous turbulence. *J. Fluid Mech.*, 225:1–20, 1991.
- [51] R. M. Kerr. Higher-order derivative correlations and the alignment of small-scale structures in isotropic numerical turbulence. *J. Fluid Mech.*, 153:31–58, 1985.
- [52] K. R. Sreenivasan and R. A. Antonia. The phenomenology of small-scale turbulence. *Annu. Rev. Fluid Mech.*, 29:435–472, 1997.



- [53] T. Ishihara, Y. Kaneda, M. Yokokawa, K. Itakura, and A. Uno. Small-scale statistics in high-resolution direct numerical simulation of turbulence: Reynolds number dependence of one-point velocity gradient statistics. *J. Fluid Mech.*, 592:335–366, 2007.
- [54] Z.-S. She, S. Chen, G. Doolen, R. H. Kraichnan, and S. A. Orszag. Reynolds number dependence of isotropic Navier-Stokes turbulence. *Phys. Rev. Lett.*, 70:3251, 1993.
- [55] A. J. Young. *Investigation of renormalization group methods for the numerical simulation of isotropic turbulence*. PhD thesis, University of Edinburgh, 1999.
- [56] W. David McComb, Arjun Berera, Matthew Salewski, and Sam R. Yoffe. An exact expression for the Reynolds number dependence of the dissipation rate in homogeneous isotropic turbulence. *arXiv:1002.2131v1[physics.flu-dyn]*, 2010.
- [57] G. K. Batchelor. *The theory of homogeneous turbulence*. Cambridge University Press, Cambridge, 1st edition, 1953.
- [58] G. Haller. An objective definition of a vortex. *J. Fluid Mech.*, 525:1–26, 2005.
- [59] J. Jeong and F. Hussain. On the identification of a vortex. *J. Fluid Mech.*, 285:69–94, 1995.
- [60] N. Okamoto, K. Yoshimatsu, K. Schneider, M. Farge, and Y. Kaneda. Coherent vortices in high resolution direct numerical simulation of homogeneous isotropic turbulence. *Phys. Fluids*, 19:115109, 2007.
- [61] J. C. R. Hunt, A. A. Wray, and P. Moin. Eddies, streams and convergence zones in turbulent flows. In *Center for Turbulence Research: Proceedings of the Summer Program*, pages 193–208, 1988.
- [62] W. D. McComb. Kolmogorov’s Theory: K41 or K62. *ERCOTAC Bulletin*, 88, 2011.
- [63] G. K. Batchelor and A. A. Townsend. The nature of turbulent motion at large wavenumbers. *Proc. R. Soc. Lond. A*, 199:238, 1949.
- [64] W. D. McComb. *The Physics of Fluid Turbulence*. Oxford University Press, 1990.
- [65] P. G. Saffman. Lectures on homogeneous turbulence. In N. Zabusky, editor, *Topics in nonlinear physics*, pages 485–614. Springer-Verlag, 1968.
- [66] R. H. Kraichnan. On Kolmogorov’s inertial-range theories. *J. Fluid Mech.*, 62:305, 1974.
- [67] A. Tsinober. *An Informal Conceptual Introduction to Turbulence*. Springer, Dordrecht, 2nd edition, 2009.
- [68] P. Sagaut and C. Cambon. *Homogeneous Turbulence Dynamics*. Cambridge University Press, Cambridge, 2008.
- [69] J. A. Domaradzki and R. S. Rogallo. Local energy transfer and nonlocal interactions in homogeneous isotropic turbulence. *Phys. Fluids A*, 2:413, 1990.
- [70] V. Shanmugasundaram. Modal interactions and energy transfers in isotropic turbulence as predicted by local energy transfer theory. *Fluid. Dyn. Res*, 10:499, 1992.

- [71] P. K. Yeung, J. G. Brasseur, and Qunzhen Wang. Dynamics of direct large-scale couplings in coherently forced turbulence: concurrent physical- and Fourier-space views. *J. Fluid Mech.*, 283:43–95, 1995.
- [72] G. K. Batchelor. *The theory of homogeneous turbulence*. Cambridge University Press, Cambridge, 2nd edition, 1971.
- [73] W. D. McComb and M. Q. May. The effect of Kolmogorov (1962) scaling on the universality of turbulence energy spectra. *arXiv:1812.09174[physics.flu-dyn]*, 2018.
- [74] W. D. McComb. *Renormalization Methods: A Guide for Beginners*. Oxford University Press, 2004.
- [75] U. Frisch. *Turbulence: the legacy of A. N. Kolmogorov*. Cambridge University Press, 1995.
- [76] G. Boffetta, A. Mazzino, and A. Vulpiani. Twenty-five years of multifractals in fully developed turbulence: a tribute to Giovanni Paladin. *J. Phys. A: Math. Theor.*, 41:363001, 2008.
- [77] H. Effinger and S. Grossmann. Static Structure Function of Turbulent Flow from the Navier-Stokes Equations. *Z. Phys. B*, 66:289–304, 1987.
- [78] H. Effinger and S. Grossmann. Prandtl number dependence of turbulent temperature structure functions: A unified theory. *Phys. Fluids A*, 1:1021–1026, 1989.
- [79] S. Grossmann and D. Lohse. Universality in fully developed turbulence. *Phys. Rev. E*, 50:2784, 1994.
- [80] J. Qian. Scaling exponents of the second-order structure function of turbulence. *J. Phys. A: Math. Gen.*, 31:3193–3204, 1998.
- [81] J. Qian. Normal and anomalous scaling of turbulence. *Physical Review E*, 58(6):7325–7329, 1998.
- [82] G. I. Barenblatt and A. J. Chorin. Turbulence: an old challenge and new perspectives. *Meccanica*, 33:445–468, 1998.
- [83] Thomas S. Lundgren. Turbulent scaling. *Phys. Fluids*, 20:31301, 2008.
- [84] David McComb. Scale-invariance in three-dimensional turbulence: a paradox and its resolution. *J. Phys. A: Math. Theor.*, 41:75501, 2008.
- [85] W. D. McComb. A modified Lin equation for the energy balance in isotropic turbulence. *Theoretical & Applied Mechanics Letters*, 10:377–381, 2020.
- [86] R. A. Antonia and P. Burattini. Approach to the 4/5 law in homogeneous isotropic turbulence. *J. Fluid Mech.*, 550:175, 2006.
- [87] J. Tchoufag, P. Sagaut, and C. Cambon. Spectral approach to finite Reynolds number effects on Kolmogorov’s 4/5 law in isotropic turbulence. *Phys. Fluids*, 24:015107, 2012.
- [88] Erik Lindborg. Correction to the four-fifths law due to variations of the dissipation. *Phys. Fluids*, 11:510, 1999.

- [89] W. D. McComb and R. B. Fairhurst. The dimensionless dissipation rate and the Kolmogorov (1941) hypothesis of local stationarity in freely decaying isotropic turbulence. *J. Math. Phys.*, 59:073103, 2018.
- [90] R. A. Antonia, L. Djenidi, L. Danilla, and S.L. Tang. Small scale turbulence and the finite Reynolds number effect. *Phys. Fluids*, 29:020715, 2017.
- [91] Shunlin Tang, Robert A. Antonia, Lyazid Djenidi, and Yu Zhou. Can small-scale turbulence approach a quasi-universal state? *Physical Review Fluids*, 4:024607, 2019.
- [92] L. Djenidi, R. A. Antonia, and S. L. Tang. Scale invariance in finite Reynolds number homogeneous, isotropic turbulence. *J. Fluid Mech.*, 864:244, 2019.
- [93] R. A. Antonia, S.L. Tang, L. Djenidi, and Y. Zhou. Finite Reynolds number effect and the 4/5 law. *Physical Review Fluids*, 4:084602, 2019.
- [94] L. Djenidi, R. A. Antonia, and S. L. Tang. Mathematical constraints on the scaling exponents in the inertial range of fluid turbulence. *Phys. Fluids*, 33:031703, 2021.